MASTERARBEIT | MASTER'S THESIS

Titel | Title

Evaluation and comparison of the immunomodulatory effects of *Alternaria* mycotoxins in immune and non-immune cells

verfasst von | submitted by

Amina Selimagic BSc

angestrebter akademischer Grad | in partial fulfilment of the requirements for the degree of

Master of Science (MSc)

Wien | Vienna, 2025

Studienkennzahl lt. Studienblatt | Degree programme code as it appears on the student record sheet:	UA 066 862
Studienrichtung lt. Studienblatt | Degree programme as it appears on the student record sheet:	Masterstudium Chemie
Betreut von | Supervisor:	Univ.-Prof. Dr. Doris Marko
Mitbetreut von | Co-Supervisor:	Dott. Dott. mag. Francesco Crudo PhD

Acknowledgments

First and foremost, I would like to express my deepest gratitude to my family, my father, my sisters, and my dear friends, whose love, patience, and understanding have made this journey lighter and more meaningful. Your unwavering support through the years has meant everything to me.

A heartfelt thank you to Vanessa, who stood by my side throughout this entire process. Together, we walked a path that was challenging for both of us, and your presence made all the difference.

I am also sincerely grateful to my colleague Noah, with whom I shared every moment in the laboratory, and to Francesco, whose kind words and encouragement lifted me during the times I doubted myself.

My deep appreciation goes to Prof. Doris Marko and all the wonderful people who were part of my master's thesis. Thank you for your guidance and for creating such an inspiring research environment.

And finally, my greatest thanks go to my husband, for his endless patience and love, and to my mother, who is sadly no longer with us.

Mama, this is for you. I love you.

List of Abbreviations

AFs	Aflatoxins
AhR	Aryl hydrocarbon receptor
ALT	Altenuene
ALTP	Alterperylenol
AME	Alternariol monomethyl ether
AMPs	Antimicrobial peptides
ANOVA	Analysis of Variance
AOH	Alternariol
APC	Antigen-presenting cell
AST	Altersetin
ATX-I	Altertoxin-I
ATX-II	Altertoxin-II
BAFFR	B-cell activating factor receptor
BCR	B-cell receptor
CCL20	Chemokine (C-C motif) ligand 20
CD	Cluster of differentiation
cDNA	Complementary DNA
C_T	Threshold cycle
CTB	CellTiter-Blue®
DAMPs	Damage-associated molecular patterns
DCs	Dendritic cells
Dex	Dexamethasone
DMEM	Dulbecco's Modified Eagle Medium
DMSO	Dimethyl sulfoxide
DNA	Deoxyribonucleic acid
dsDNA	Double-stranded DNA
dNTPs	Deoxynucleoside triphosphates
EDTA	Ethylenediaminetetraacetic acid
EFSA	European Food Safety Authority
EGF	Epidermal Growth Factor
ELISA	Enzyme Linked Immunosorbent Assay
ER	Estrogen receptor
FBS	Fetal bovine serum

GALT	Gut-associated lymphoid tissue
GIT	Gastrointestinal tract
GM-CSF	Granulocyte-macrophage colony-stimulating factor
IBD	Inflammatory bowel disease
IEB	Intestinal epithelial barrier
IEC	Intestinal epithelial cells
IgA	Immunoglobulin A
IKK	IκB kinase
IL	Interleukins
LAL	Limulus amebocyte lysate
LC-MS/MS	Liquid chromatography/tandem mass spectrometry
LPO	Lipid peroxidation
LPS	Lipopolysaccharide
LTßR	Lymphotoxin beta receptor
MCP-1	Monocyte chemoattractant protein-1
M-CSF	Macrophage colony-stimulating factor
MD2	Myeloid differentiation factor 2
MMP-2	Matrix metallopeptidase 2
mRNA	Messenger RNA
NEMO	NF-κB essential modulator
NF-κB	Nuclear factor kappa B
NIK	NF-κB-inducing kinase
NK	Natural killer
P/S	Penicillin/Streptomycin
PAMPs	Pathogen-associated molecular patterns
PBS	Phosphate buffered saline
PCR	Polymerase chain reaction
PKC	Protein kinase C
PMA	Phorbol 12-myristate 13-acetate
PRRs	Pattern-recognition receptors
qRT-PCR	Quantitative real-time polymerase chain reaction
RA	Rheumatoid arthritis
RANK	Receptor activator of nuclear factor κB
RASFF	Rapid Alert System for Food and Feed
RHD	Rel homology domain

RNA	Ribonucleic acid
ROS	Reactive oxygen species
RPMI 1640	Roswell Park Memorial Institute medium 1640
RT	Reverse transcription
SD	Standard deviation
sIgA	Secretory immunoglobulin A
SRB	Sulforhodamine B
TCR	T-cell receptor
TEER	Transepithelial electrical resistance
TEN	Tentoxin
TGF	Transforming growth factor
Th	T helper
TLR	Toll Like receptor
T_m	Melting temperature
TNF-α	Tumor necrosis factor α
TTC	Thresholds of Toxicological Concern
WST-1	Water-soluble tetrazolium salt 1

Abstract

The frequent occurrence of *Alternaria* mycotoxins in food, coupled with their diverse spectrum of toxic effects, underscores their potential to significantly impact human health. Nevertheless, comprehensive data on the immunomodulatory effects of the majority of these contaminants are still missing. The present study aimed to investigate the immunomodulatory effects of *Alternaria* mycotoxins in lipopolysaccharide (LPS)-induced immune cells (THP-1 Lucia™ monocytes and THP-1 Lucia™ macrophages) and interleukin 1β (IL-1β)-induced non-immune cells (cancerous Caco-2 cells and noncancerous HCEC-1CT cells), and to contribute to closing the data gaps, assess their risk in consumed food, and ultimately lead to their regulation.

Altenuene (ALT) and tentoxin (TEN) were described for the first time as immunosuppressive compounds in THP-1 Lucia™ monocytes and in THP-1 Lucia™ macrophages, where in monocytes they suppressed the activation of the NF-κB signaling pathway at concentrations ≥ 5 µM and ≥ 2 µM, respectively. While ALT exhibited the same effect in THP-1 Lucia™ macrophages, TEN was slightly less potent, inducing suppression starting at 5 µM. Alternariol (AOH), alternariol monomethyl ether (AME), altersetin (AST), alterperylenol (ALTP) and altertoxin-I (ATX-I) were tested only in THP-1 Lucia™ macrophages showing immunomodulatory effects: AOH (≥ 1 µM), AME (≥ 0.01 µM), AST (≥ 0.1 µM), ALTP (≥ 1 µM), ATX-I (≥ 5 µM).

Because intestinal epithelial cells (IECs) are subjected to high concentrations of ingested mycotoxins, the potential for immunomodulatory effects at the gastrointestinal barrier should be taken into account. In addition to the already known immunosuppressive effect of AOH on Caco-2 and HCEC-1CT cells, ALTP was the only tested mycotoxin to show immunomodulatory properties and was thus for the first time characterized as an immunosuppressive compound in IECs. It caused downregulation in the expression of the pro-inflammatory cytokines IL-8 and TNF-α at ≥ 5 µM in Caco-2 cells, while IL-6 expression was decreased at 10 µM. In HCEC-1CT cells, ALTP demonstrated the downregulation of IL-6, IL-8 and TNF-α starting with a concentration of 1 µM.

It can be summarized that all tested mycotoxins exhibit immunomodulatory properties in immune cells, whereas effects on the intestinal epithelial barrier (IEB) are observed only for ALTP in addition to AOH. These results indicate the immunosuppressive potential of *Alternaria* mycotoxins and their possible impact on immune system regulation. Further studies are needed to clarify their underlying mechanisms of action and to comprehensively assess the risks they pose to human health.

Zusammenfassung

Das häufige Vorkommen von *Alternaria*-Mykotoxinen in Lebensmitteln, zusammen mit ihrem breiten Spektrum toxischer Wirkungen, unterstreicht ihr Potenzial, die menschliche Gesundheit erheblich zu beeinträchtigen. Dennoch fehlen umfassende Daten zu den immunmodulatorischen Effekten der meisten dieser Kontaminanten. Die vorliegende Studie hatte zum Ziel, die immunmodulatorischen Effekte von *Alternaria*-Mykotoxinen in lipopolysaccharid (LPS)-induzierten Immunzellen (THP-1 Lucia™-Monozyten und THP-1 Lucia™-Makrophagen) sowie in interleukin-1β (IL-1β) -induzierten Nicht-Immunzellen (kanzeröse Caco-2-Zellen und nicht-kanzeröse HCEC-1CT-Zellen) zu untersuchen, um Datenlücken zu schließen, ihr Risiko in verzehrten Lebensmitteln zu bewerten und letztlich ihre Regulierung zu unterstützen.

Altenuen (ALT) und Tentoxin (TEN) wurden erstmals als immunsuppressive Verbindungen in THP-1 Lucia™-Monozyten und THP-1 Lucia™-Makrophagen beschrieben, wobei sie in Monozyten die Aktivierung des NF-κB-Signalwegs bei Konzentrationen von ≥ 5 µM bzw. ≥ 2 µM unterdrückten. Während ALT denselben Effekt in THP-1 Lucia™-Makrophagen zeigte, war TEN etwas weniger wirksam und induzierte eine Suppression ab 5 µM. Alternariol (AOH), Alternariolmonomethylether (AME), Altersetin (AST), Alterperylenol (ALTP) und Altertoxin-I (ATX-I) wurden ausschließlich in THP-1 Lucia™-Makrophagen getestet und zeigten immunmodulatorische Effekte: AOH (≥ 1 µM), AME (≥ 0,01 µM), AST (≥ 0,1 µM), ALTP (≥ 1 µM), ATX-I (≥ 5 µM).

Da Darmepithelzellen (IECs) hohen Konzentrationen aufgenommener Mykotoxine ausgesetzt sind, sollte das Potenzial für immunmodulatorische Effekte an der gastrointestinalen Barriere berücksichtigt werden. Neben der bereits bekannten immunsuppressiven Wirkung von AOH auf Caco-2- und HCEC-1CT-Zellen zeigte nur ALTP immunmodulatorische Eigenschaften und wurde somit erstmals als immunsuppressive Verbindung in IECs charakterisiert. Es verursachte eine Herunterregulierung der Expression der proinflammatorischen Zytokine IL-8 und TNF-α bei ≥ 5 µM in Caco-2-Zellen, während die IL-6-Expression bei 10 µM reduziert wurde. In HCEC-1CT-Zellen zeigte ALTP eine Herunterregulierung von IL-6, IL-8 und TNF-α bereits ab einer Konzentration von 1 µM.

Zusammenfassend lässt sich sagen, dass alle getesteten Mykotoxine immunmodulatorische Eigenschaften in Immunzellen aufweisen, während Effekte auf die intestinale Epithelbarriere (IEB) nur für ALTP zusätzlich zu AOH beobachtet wurden. Diese Ergebnisse deuten auf das immunsuppressive Potenzial von *Alternaria*-Mykotoxinen und ihre mögliche Auswirkung auf die Regulation des Immunsystems hin. Weitere Studien sind erforderlich, um ihre grundlegenden Wirkmechanismen zu klären und die von ihnen ausgehenden Risiken für die menschliche Gesundheit umfassend zu bewerten.

Table of Content

1 Introduction

This introduction provides an overview of the most relevant mycotoxins, with a particular focus on *Alternaria* toxins, their occurrence, chemical characteristics, toxicological effects, and their impact on the immune system and the intestinal epithelial barrier (IEB).

1.1. Mycotoxins

Mycotoxins are toxic secondary metabolites produced by various filamentous fungi, primarily those belonging to the genera *Aspergillus*, *Penicillium*, *Alternaria*, *Fusarium*, and *Claviceps* [1,2].Among the most relevant mycotoxins are the aflatoxins (AFs), produced by *Aspergillus* species. Ochratoxin A represents another major threat, as it can be synthesized by both *Aspergillus* and *Penicillium*. *Fusarium* species, on the other hand, are well known for their remarkable versatility, giving rise to a wide array of toxic metabolites including trichothecenes, zearalenone, and fumonisins B1 and B2. Finally, the ergot alkaloids originate from *Claviceps* species [3]. The contamination of food by mycotoxins is considered a global and unpredictable issue, as it can occur even when good agricultural practices are applied, posing a major challenge to food safety [1]. Various climate changes, such as increased CO_2 concentrations, changes in temperature, precipitation, and water availability, are among the factors that can lead to an unexpected increase in crop contamination with mycotoxins. Due to global warming, the emergence of new diseases and changes in fungal biodiversity and microbiomes may occur [4]. Many food products can be contaminated with mycotoxins, such as coffee, cereals, dried fruit, and spices. Due to the structural diversity of mycotoxins, the effects these compounds can cause, and their high chemical stability, efficient detection methods are necessary [5]. Due to their potential impact on consumer health, many countries have implemented regulations to limit exposure to mycotoxins. According to the annual report of the Rapid Alert System for Food and Feed (RASFF), in 2012, mycotoxins represented the most frequently reported hazard in border rejection notifications within the European Union. AFs were the primary cause of these notifications, mainly due to exceeding the maximum permitted levels with dried figs being a frequent source of contamination. Additionally, the presence of ochratoxin A, particularly in spices and medicinal herbs, also led to rejections due to levels exceeding the allowed limits [6]. Several mycotoxins, including ochratoxin A, aflatoxin B1, and deoxynivalenol, are regulated in the European Union under the Contaminants Regulation (Regulation (EU) 2023/915), which sets maximum permitted levels for some of the most relevant mycotoxins [7]. In contrast, other mycotoxins, such as enniatins,

beauvericin, moniliformin, as well as *Alternaria* mycotoxins are not regulated due to insufficient toxicological and occurrence data, although they are increasingly being detected in food [8].

1.2. *Alternaria* toxins

Fungi of the genus *Alternaria* are ubiquitous plant pathogens and saprophytes, widely distributed in nature. Crops can become infected both in the field and during the postharvest stage, resulting in the rot of fruits and vegetables and significant food losses. Plant diseases negatively affect the agricultural economy by reducing both the yield and quality of crops, vegetables, and fruits. *Alternaria* species synthesize various toxic metabolites during their active growth, which cause severe diseases in numerous plants and significantly reduce their yield [9].The so-called *Alternaria* mycotoxins can migrate from decayed tissue to surrounding areas, which is why they are also found in processed food products [10–12].

1.2.1. Classification

The *Alternaria* genus comprises various species, including *A. alternata*, *A. tenuissima*, *A. arborescens*, *A. radicina*, *A. brassicae*, *A. brassicicola*, and *A. infectoria*. The *Alternaria* species that most commonly produces mycotoxins is *A. alternata*. The key *Alternaria* mycotoxins were initially isolated, identified, and confirmed between 1953 and 1986 [10,11]. Various secondary toxic metabolites with distinct chemical structures can be produced and based on these structures, they can be classified into different groups. As shown in Figure 1, the mycotoxins examined in this master's thesis are categorized into three groups: dibenzo-α-pyrones, perylene quinones and *Alternaria* mycotoxins with miscellaneous structures. Dibenzo-α-pyrones include, among others, alternariol (AOH), alternariol monomethyl ether (AME), and altenuene (ALT). Perylene quinones include altertoxin I (ATX-I) and alterperylenol (ALTP), whereas altersetin (AST) and tentoxin (TEN) can be categorized as *Alternaria* mycotoxins with miscellaneous structures [11,13].

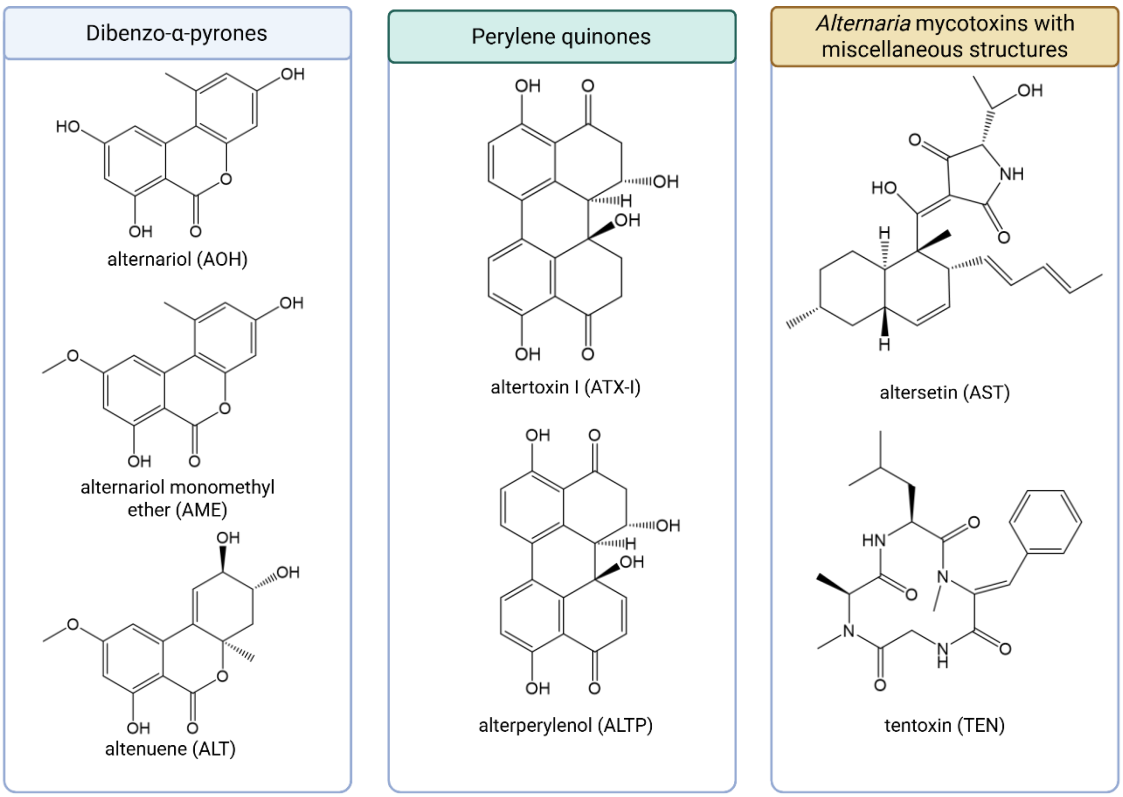

Figure 1: Grouping and structures of *Alternaria* mycotoxins: alternariol (AOH), alternariol monomethyl ether (AME), altenuene (ALT), altertoxin-I (ATX-I), alterperylenol (ALTP), altersetin (AST) and tentoxin (TEN) (Created in https://BioRender.com and ChemSketch)

1.2.2. Occurrence

Alternaria mycotoxins can be found in various fresh as well as processed food products. They are most commonly present in fruits, vegetables, fermented beverages, and various cereals. Among vegetables, tomatoes and tomato-based products are particularly notable [12]. Formation of *Alternaria* mycotoxins can occur at various stages, including in the field, during harvest, transportation and storage. *Alternaria* fungi grow at specific temperatures, between 22–28 °C, but growth is also possible at temperatures as low as -3 °C. This means that these fungi can grow both at room temperature in various climate zones as well as under cold storage conditions [14].In a study investigating contamination levels of food and feed, the detected concentration of most mycotoxins of this genus in cereals were below 100 µg/kg, with maximum concentrations not exceeding 1000 µg/kg. Moreover, although *Alternaria* toxins were not detected in fresh tomatoes, the majority of processed tomato products contained at least one mycotoxin from this group. Additionally, these toxins were found in fruit juices and wines, where concentrations were generally low, typically in the range of a few µg/l. However, the limited number of analyzed samples may represent a bias that affects the detection of less frequently occurring toxins [15]. In 2011, the European Food Safety Authority (EFSA) established Thresholds of Toxicological Concern (TTC) values only for certain *Alternaria* mycotoxins. For AOH and AME, the TTC value for

chronic dietary exposure was set to 2.5 ng/kg body weight per day. Due to the lack of evidence for genotoxicity, the TTC value for TEN was set to 1.5 µg/kg body weight per day [12]. However, due to the lack of toxicological data, *Alternaria* mycotoxins are still not regulated and are classified as "emerging mycotoxins" [8].

1.2.3. Characteristics, exposure and toxicity of selected *Alternaria* mycotoxins

The following section deal with individual *Alternaria* mycotoxins within the scope of this thesis, with a particular focus on their chemical characteristics, exposure levels, toxic effects, and the currently available data relevant to human health risk assessment.

1.2.3.1. Alternariol, alternariol monomethyl ether and altenuene

AOH and AME are one of the most extensively studied mycotoxins of the genus *Alternaria* and they are often investigated together due to their similarities in chemical structure [16]. The most significant dietary source of AOH are fruit and fruit products, while AME can be found in several types of cereal grains, such as wheat, barley, and sorghum. However, due to the low consumption of these grains, their contribution to overall exposure is minimal [17]. AOH and AME are known to cause genotoxicity in colon carcinoma cells, as well as cytotoxicity and genotoxicity in liver cell models [16,18]. AME exhibits certain toxic effects in both humans and animals, including cytotoxic activity on bacterial and mammalian cells, as well as fetotoxicity and teratogenicity in mice and hamsters [19]. AOH exhibited a growth-inhibitory effect in HT29 cells in a concentration-dependent manner, which was associated with increased production of reactive oxygen species (ROS) [20]. Moreover, due to their structural similarity to 17β-estradiol (E2), both toxins exhibit endocrine-disrupting potential by binding to and activating estrogen receptors (ER) [16].Furthermore, AOH has been shown to upregulate progesterone receptor expression and enhance the production of estradiol and progesterone in the H295R cell line, underlining its potential as an endocrine-disrupting compound [21]. In addition to genotoxic, cytotoxic, and endocrine-disrupting effects, the impact of these mycotoxins on the immune system and their immunotoxicological activity have been investigated in several studies; however, the available data remains limited. Current findings indicate that AOH suppresses lipopolysaccharide (LPS)-induced inflammation in THP-1 derived macrophages [22]. Moreover it exhibits immunosuppressive effects in differentiated Caco-2 cells stimulated with interleukin 1β (IL-1β) [23]. The ability of these two dibenzo-α-pyrones to modulate innate immunity was also investigated in the human bronchial epithelial cell line (BEAS-2B) and the murine macrophage cell line (RAW264.7), where AOH was shown to exert strong, concentration-dependent immunosuppressive activity in both cell lines. In detail, significant suppression of LPS-induced IL-8 was observed already at a dose of 5 µM. AME was

also found to suppresses innate immune responses at a concentration of 10 µM , but to a lesser extent compared to AOH [24]. Although it belongs to the same group of mycotoxins as AOH and AME, data on the occurrence and toxicity of ALT remain very limited. ALT can be found in alcoholic beverages, fruit and vegetable juices, grains and grain-based products, and others [12]. Current toxicological data show that ALT exhibits strong cytotoxicity in the cancer cell line HCT116, as determined by the sulforhodamine B (SRB) colorimetric assay after 72 h of incubation, with an IC_{50} value of 3.13 µM, which is comparable to that of the positive control etoposide (IC_{50}=2.13 µM) [25]. However, studies on the effects of ALT on the immune system are still lacking.

1.2.3.2. Altertoxin-I and alterperylenol

The perylene quinone ATX-I can be found in fruit and fruit products, oilseed meals, vegetables, and vegetable products. However, occurrence data for ALTP and dietary exposure for this mycotoxin are still lacking. Currently, such data are only available for a few *Alternaria* mycotoxins [12,26]. Regarding toxicological information, no studies have yet investigated the genotoxicity of ATX-I [13]. In contrast, ALTP has demonstrated significant cytotoxic activity in various tumor cell lines, including MCF-7, HepG2, NCI-H460, and SF-268, with IC_{50} values ranging from 1.91 to 9.67 µM. Cytotoxic activity was evaluated using the SRB assay, with cisplatin used as a positive control [27]. The mutagenicity of ATX-I, both with and without nitrosylation, was evaluated using the Ames test with *Salmonella* strains TA98 and TA100. Without nitrosylation, ATX-I demonstrated mutagenic activity at concentrations ranging from 1 to 100 µg/plate in TA98 when metabolically activated with rat liver S9 fraction. Co-incubation with nitrite enhanced the mutagenic effect-with or without S9 activation-in both strains, TA98 and TA100 [28]. Regarding immunotoxicity, the *Alternaria* mycotoxins ALTP and ATX-I have shown immunosuppressive properties in THP-1 Lucia™ monocytes by inhibiting LPS-induced activation of the kappa-light-chain-enhancer of activated B cells (NF-κB) pathway at concentrations ≥ 1 µM. In addition to being newly identified immunosuppressive compounds, ALTP and ATX-I also exhibit antiestrogenic effects. In Ishikawa cells, ALTP (≥ 0.4 µM) and ATX-I (≥ 2 µM) suppressed estrogen-dependent expression of enzyme activity [29].

1.2.3.3. Tentoxin and altersetin

Available data on the toxicological properties and occurence of TEN and AST are limited. TEN has most frequently been detected in oilseeds, cereals, cereal milling products, and tree nuts [17], whereas data on the occurrence of AST in food are still lacking. Currently, there are only a few studies addressing the toxicity of these mycotoxins. The genotoxicity of TEN was investigated in HEK293T cells, where it did not induce statistically significant DNA strand breaks [30]. Using liquid

chromatography/tandem mass spectrometry (LC-MS/MS), AST was identified in the *Alternaria* extract. Its immunomodulatory properties were investigated in THP-1 Lucia™ monocytes using the NF-κB reporter gene assay, where it showed immunoinhibitory effects at concentrations ≥2 µM. In addition, it exhibited antiestrogenic properties in Ishikawa cells at concentrations ≥5 µM [31].

1.3. The immune system

The immune system protects the body from foreign antigens and is divided into two types of defense: innate (natural) and adaptive (acquired) immunity. Innate immunity is an antigen-independent defense mechanism, meaning it reacts immediately and does not have the ability to recognize the same pathogen upon repeated exposure. This function is carried out by phagocytic cells such as macrophages. In contrast, adaptive immunity is antigen specific, and it has immunological memory, enabling it to respond more rapidly upon subsequent exposure to the same pathogen [32–34]. When the innate immune response is insufficient to control the infection, the adaptive immune system is activated. In such cases, the innate immune system relays critical information about the nature of the pathogen to guide the adaptive response [35].

The immune system functions by producing many cells generated in the bone marrow after early childhood. Certain proteins are located on the cell membrane of white blood cells. Among these proteins are receptors that enable the cells to communicate with each other and interact with their environment. Receptors bind ligands, such as soluble molecules like cytokines, thereby transmitting signals that regulate immune responses [35,36]. Cells use a system to examine the proteins they have bound and, if some originate from a virus, they produce cytokines and release cellular remnants that can initiate an adaptive immune response [36].

The innate immune system recognizes microorganisms that can lead to infection through pattern-recognition receptors (PRRs), such as Toll Like receptors (TLRs). By recognizing different microbial components, the innate immune system activates immune cells, which then initiate intracellular signalling pathways such as canonical NF-κB pathway. As LPS is known to induce NF-κB activation by binding to PRRs, particularly TLR4, this activation triggers the expression of genes encoding proinflammatory cytokines such as tumor necrosis factor (TNF), IL-1, and IL-6 and chemokines [32]. Through the production of cytokines and chemokines-small signaling proteins involved in intercellular communication and cell migration-the innate immune system rapidly recruits immune cells to sites of infection and inflammation. Among the most important inflammatory cytokines released in the early phase of bacterial infection are TNF, IL-1, and IL-6. Conversely, dysregulated production of these proinflammatory cytokines is associated with

chronic inflammatory and autoimmune diseases, making them important therapeutic targets [33,37,38].Cells that express innate immune receptors include macrophages, dendritic cells (DCs), mast cells, neutrophils, eosinophils, and natural killer (NK) cells. Once activated, they rapidly differentiate into effector cells whose primary role is to eliminate infection [35]. These cells express PRRs, which detect pathogen-associated molecular patterns (PAMPs) and damage-associated molecular patterns (DAMPs) [37].

Monocytes originate in the bone marrow and are continuously released into the bloodstream. When recruited by chemotactic molecules, they become activated and differentiate into macrophages under the influence of mediators such as macrophage colony-stimulating factor (M-CSF) and phorbol 12-myristate 13-acetate (PMA). In addition to their crucial role in host defence, these cells, together with neutrophils, act as phagocytic cells, helping to eliminate microorganisms [39,40]. Beyond their role as phagocytes, circulating monocytes provide effective protection against bacterial infections, including those caused by Gram-negative bacteria. When exposed to LPS, a potent endotoxin, peripheral monocytes migrate to the lymph nodes, where they differentiate into DCs. DCs "display" bacterial fragments (antigens) to T lymphocytes. CD4+ T helper cells coordinate the immune response by activating B lymphocytes for antibody production and by stimulating other immune cells, while CD8+ cytotoxic T cells directly kill infected host cells. In this way, DCs serve as a bridge between the innate and adaptive immune system. However, human peripheral blood monocytes differ from THP-1 cells, which are used as a model for primary monocytes. Primary monocytes are significantly more responsive due to the high expression of cluster of differentiation 14 (CD14), a co-receptor for TLRs that forms a highly sensitive LPS signaling complex (CD14–TLR4–MD2).

Under various conditions, activated macrophages can differentiate into M1 or M2 subsets. M1 macrophages produce proinflammatory cytokines such as IL-1, IL-6, IL-12, and TNF-α, and promote differentiation of T helper cell 1 (Th1) and Th17, which further drive inflammation. In contrast, M2 macrophages secrete anti-inflammatory cytokines such as IL-10 and IL-13 and are essential for reducing inflammation and promoting tissue repair [37].

1.3.1. Nuclear factor kappa B signaling pathway

NF-κB, is a transcription factor, involved in various cellular processes such as cell proliferation, apoptosis, neuronal development, and also plays a key role in regulating inflammatory responses. The NF-κB family includes five members: p65 (RelA), RelB, c-Rel, NF-κB1 (p50), and NF-κB2 (p52). All members are capable of forming homo-or heterodimers. A common feature of these proteins is the Rel Homology Domain (RHD), which enables dimerization. In the form of

homo-or heterodimers, they bind to specific DNA elements known as κB enhancers. With the help of inhibitory proteins (IκBs), of which the most important is IκBα, NF-κB proteins are retained in the cytoplasm in their inactive state.

NF-κB activation occurs through the canonical and non-canonical pathways. The canonical NF-κB signaling pathway is activated by various stimuli such as proinflammatory cytokines, e.g., TNF-α and IL-1β, ligands of PRRs, and antigen receptors such as the T-cell receptor (TCR) and B-cell receptor (BCR). The core mechanism of canonical NF-κB activation is inducible degradation of IκBα. This degradation occurs through site-specific phosphorylation by the IκB kinase (IKK) complex. The IKK complex consists of IKKα and IKKβ, which serve as two catalytic subunits, and the NF-κB essential modulator (NEMO, also known as IKK), which is the regulatory subunit. First, the IKK complex is activated by various stimuli such as cytokines. It then phosphorylates IκBα at two N-terminal serine residues, leading to its ubiquitin-dependent degradation by the proteasome. This allows the release of NF-κB proteins, predominantly p65, which translocate to the nucleus with the help of importin proteins, such as importin α3 and importin α4. There, the homo-or heterodimers bind to DNA and initiate activation of immune response genes (see Figure 2). The canonical NF-κB signaling pathway is active in almost all cells of the innate and adaptive immune systems.

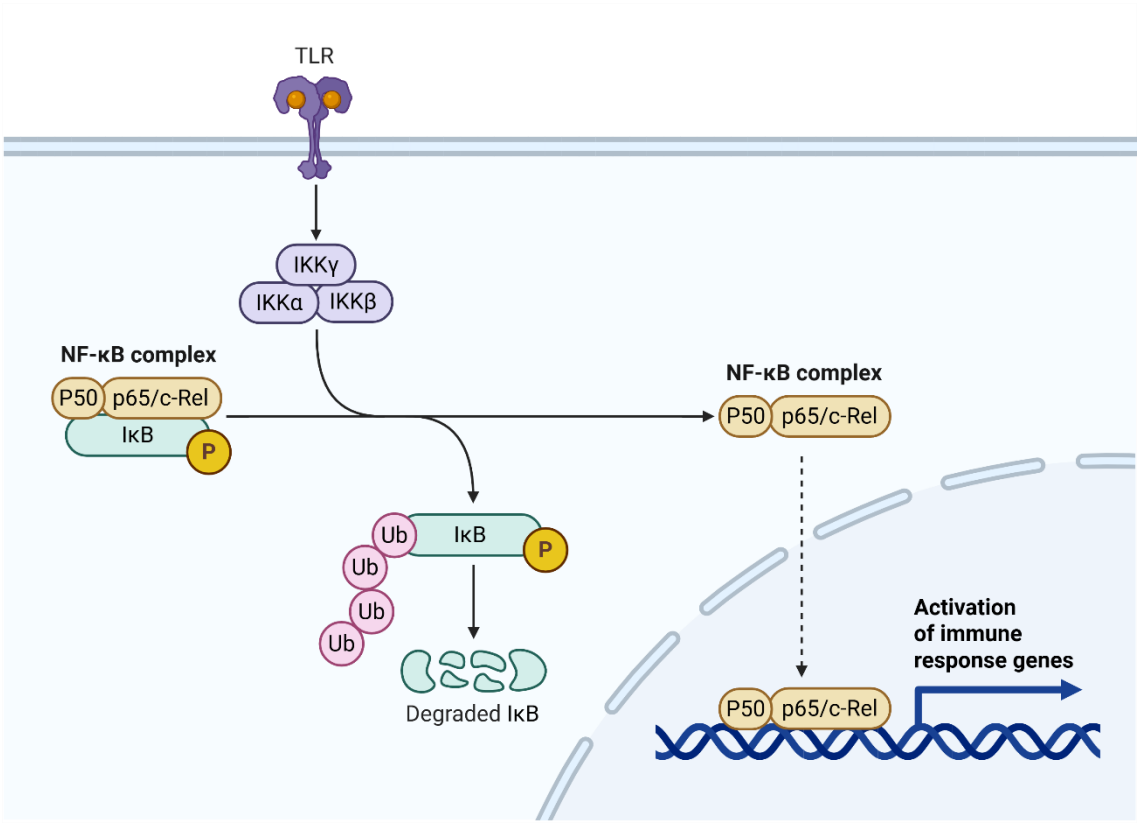

Figure 2: NF-κB signaling pathway (Created in https://BioRender.com)

In contrast, the non-canonical pathway, only responds to a specific group of stimuli, such as the activation of lymphotoxin beta receptor (LTβR), B-cell activating factor receptor (BAFFR), CD40,

and receptor activator of nuclear factor κB (RANK). This pathway is based on the processing of the precursor protein p100, with the NF-κB-inducing kinase (NIK) playing a key role. NIK is a crucial signaling molecule. To phosphorylate p100, NIK activates IKKα, which then leads to ubiquitination and processing. Processing of p100 involves the degradation of its C-terminal IκB-like domain. This results in the formation of p52, which supports the nuclear translocation of the p52/RelB complex and the subsequent expression of specific target genes. Unlike the canonical pathway, the non-canonical pathway plays a role in regulating functions of the adaptive immune system.

Through these mechanisms, NF-κB acts as a central mediator of inflammation. Its activation leads to the production of proinflammatory cytokines, such as TNF-α, IL-1, and IL-6, chemokines, and adhesion molecules, while the resolution of inflammation involves anti-inflammatory mediators, including IL-10, TGF-β, and lipoxins. This balance ensures both effective host defense and tissue regeneration. Dysregulation of NF-κB signaling, however, contributes to chronic inflammatory and autoimmune diseases, such as rheumatoid arthritis (RA) and inflammatory bowel disease (IBD) [37,41–43].

1.3.2. Impact of mycotoxins on NF-κB signaling pathway

Various mycotoxins have shown an impact on the immune system and the NF-κB signaling pathway in general. In addition to the effect of AOH, ATX-I, ALTP and AST [22,29,31] on the suppression of the NF-κB signaling pathway, the impact of the *Alternaria* mycotoxin altertoxin-II (ATX-II) was also investigated in THP-1 macrophages, where ATX-II at non-cytotoxic concentrations inhibited the activation of the transcription factor NF-κB [44]. In addition to *Alternaria* mycotoxins, zearalenone, which is produced by *Fusarium* species, reduced the expression of pro-and anti-inflammatory mediators and mitogen-activated protein kinase/NF-κB signaling molecules in the liver of pigs [45]. Due to its structural similarity to deoxynivalenol, the trichothecene NX-3 was investigated in human colon cell lines, including non-cancerous HCEC-1CT cells and cancerous HT-29 cells. NX-3 and deoxynivalenol significantly activated an NF-κB-regulated reporter gene under pro-inflammatory conditions (IL-1β-induced) and increased the expression of genes encoding pro-inflammatory cytokines (IL-8, IL-6, TNF-α, and IL-1β) [46].

1.4. The intestinal epithelial barrier

The gastrointestinal tract (GIT) is one of the largest interfaces between the external environment and the body's internal systems. A critical component of this interface is the IEB which is a dynamic structure that acts as the body's primary defence mechanism against harmful

microorganisms and antigens. The IEB plays a dual role: it protects the deeper layers of the intestinal wall while facilitating essential physiological processes, such as the absorption of nutrients, water and ions. This balance is maintained through a coordinated interaction between several elements: outermost mucus layer, a single layer of epithelial cells and the underlying lamina propria. The underlying lamina propria contains immune cells such as DCs, lymphocytes, macrophages, and others.

Tight junctions between epithelial cells form adhesive intercellular complexes that polarize the intestinal epithelium and regulate selective ion transport. Transport across the epithelium occurs through paracellular, transcellular, transporter-mediated, and endocytic routes, depending on the properties of the molecules involved [47].

The intestinal epithelium is composed of five main cell types, namely absorptive enterocytes, goblet cells, tuft cells, enteroendocrine cells, and Paneth cells. Goblet cells produce mucus that prevents microbial adhesion, whereas Paneth cells secrete antimicrobial peptides (AMPs) that disrupt bacterial membranes. Plasma cells produce secretory immunoglobulin A (sIgA) in the lamina propria. The sIgA is then transported through the epithelial cells into the lumen, where it blocks pathogen receptors. These elements work collectively to maintain homeostasis and immune surveillance. Disruption of the IEB, often referred to as increased intestinal permeability or "leaky gut," can allow antigens and microbes to penetrate into the lamina propria. This intrusion may lead to immune system activation and sustained inflammatory responses, which are associated with the development of various disorders [40,47].

The GIT also contains specialized gut-associated lymphoid tissue (GALT), the body's largest peripheral lymphoid tissue. The GALT includes Peyer's patches and mesenteric lymph nodes, which serve as inductive sites for intestinal immunity. M cells, a specialized epithelial subtype, capture microbial antigens from the lumen and deliver them to underlying immune tissues, initiating both mucosal and systemic immune responses. The intestinal immune system must strike a balance between tolerance to commensal microbiota and effective responses to pathogenic threats. This balance is maintained by inductive sites like GALT and effector sites such as the lamina propria and intestinal epithelium, where activated immune cells maintain barrier integrity and immunity [48]. When homeostasis is disrupted, epithelial cells interact with immune cells to mediate inflammatory responses. The production of pro-and anti-inflammatory cytokines is finely regulated during inflammation. Intestinal epithelial cells (IECs) produce cytokines such as IL-1β, which plays a critical role in both acute and chronic inflammation. Other cytokines constitutively expressed in IECs include TGF-α, IL-10, IL-15, and IL-18, contributing to immune cell influx and epithelial homeostasis. Expression of IL-1α/β, IL-6, IL-8, TNF-α, monocyte

chemoattractant protein-1 (MCP-1), chemokine (C-C motif) ligand 20 (CCL20), and granulocyte-macrophage colony-stimulating factor (GM-CSF) increases significantly during microbial infections, highlighting IECs' central role in immune regulation [49,50].

In conclusion, the IEB plays a crucial role in maintaining gastrointestinal health by ensuring structural integrity, immunological function, and regulated permeability. Disruptions in this complex system can lead to pathological inflammation and disorders such as IBD, underlining the importance of ongoing research into IEC function and intestinal immunity [47].

1.4.1. Impact of mycotoxins on the IEB

Given that the GIT is the primary target for toxic substances, the effects of many mycotoxins on the intestinal epithelium have been widely studied. In addition to the immunosuppressive effects of AOH on IL-1β-stimulated, differentiated Caco-2 cells[23], the impact of other *Alternaria* mycotoxins on intestinal cells has also been investigated. Among others, ATX- II was studied in intestinal cells, cancerous HT-29 cells line and non-cancerous epithelial cell line HCEC-1CT, where it was shown that even short-term exposure of intestinal cells the mycotoxin is sufficient to impair their functionality. In HCEC-1CT cells, it disrupted key functions related to cellular regeneration and the barrier function of healthy intestinal cells [51]. Furthermore, in HCEC-1CT cells, AOH and ATX-II suppressed mRNA levels of the proinflammatory mediators IL-8 and TNF-α, as well as IL-8 secretion and mRNA levels of matrix metallopeptidase 2 (MMP-2). Both toxins also repressed the intestinal immune response at the protein level [50]. In addition, mycotoxins from the genera *Aspergillus*, *Fusarium*, and others have also been investigated. Deoxynivalenol is a mycotoxin of the trichothecene family, mainly produced by *F. graminearum* and *F. culmorum*, and has been studied in intestinal epithelial cell lines of porcine (IPEC-1) or human (Caco-2) origin, where it caused a decrease in transepithelial electrical resistance (TEER). Deoxynivalenol also disrupted claudin expression and impairs the function of the IEB [52]. Additionally, ochratoxin induced intestinal barrier dysfunction and tight junction disruption in IPEC-J2 cell monolayers [53]. Aflatoxin B1, fumonisin B1, ochratoxin A, and T-2 toxin have been shown to be cytotoxic to Caco-2 cells, significantly disrupting monolayer integrity and reducing the expression of claudin-3, claudin-4, and occludin in this cell line [54]. Additionally, at low doses zearalenone stimulated the proliferation of colon cancer cells (HCT116), whereas at high doses, it induced cytotoxicity [55]. Many other studies have addressed mycotoxins and their impact on the IEB in the past, as they remain a subject of ongoing research.

2 Aims and Objectives

Alternaria mycotoxins produced, by species of the genus *Alternaria*, are, structurally diverse secondary metabolites frequently found in food, and some of them may potentially pose a threat to human health [11]. Although several toxic effects, such as genotoxic, cytotoxic, and endocrine-disrupting activities, have already been described, their immunomodulatory properties remain insufficiently investigated. Due to the limited toxicological data available, *Alternaria* mycotoxins are not yet regulated in the European Union and are therefore classified as “emerging mycotoxins" [15].

The aim of this thesis was therefore to investigate the immunomodulatory effects of selected *Alternaria* mycotoxins in both immune and non-immune cells thereby contributing to a better understanding of their biological activity and supporting future risk assessment and regulatory considerations. To this end the effects of different mycotoxins on the NF-κB signaling pathway were examined in LPS-stimulated THP-1 Lucia™ monocytes (ALT and TEN) and in LPS-induced THP-1 Lucia™ macrophages (AOH, AME, ALT, ATX-I, ALTP, AST and TEN) using the NF-κB reporter gene assay. THP-1 Lucia™ cells were selected for their sensitivity to inflammatory stimuli and their ability to mimic aspects of the human innate immune response. In parallel, the CellTiter-Blue®(CTB) assay was employed to assess cytotoxicity and to exclude the possibility that immunomodulatory effects were secondary due to cytotoxicity. As oral intake is the main route of exposure, the GIT represents a primary target of *Alternaria* mycotoxin toxicity. Furthermore, while immune cells are critical mediators of the host’s response to mycotoxins, their activation is tightly regulated, among other factors, by signals from IECs. IECs not only serve as the primary barrier against ingested toxins but also participate in NF-κB-dependent crosstalk with immune cells. Therefore, the second part of this thesis focused on the impact of the same mycotoxins on the IECs Caco-2 and HCEC-1CT. Here, the expression of pro-inflammatory cytokines (IL-6, IL-8, TNF-α) and the anti-inflammatory cytokine IL-10 was analyzed at the mRNA level in IL-1β-stimulated cells using quantitative real-time polymerase chain reaction (qRT-PCR). These cell lines were chosen to reflect both cancerous (Caco-2) and non-cancerous (HCEC-1CT) intestinal epithelium. Again, only non-cytotoxic concentrations were applied, as determined by the CTB assay, to ensure reliable interpretation of the results.

Taken together, this thesis aimed to contribute to a better understanding of the immunomodulatory potential of *Alternaria* mycotoxins in relevant cellular models, thereby closing existing data gaps and contributing to their toxicological characterization in the context of food safety.

3 Materials

In the following, the chemicals, reagents, materials, instruments and software used for the experiments are listed.

3.1. Cell lines and cell culture reagents

Table 1: Cell lines

Cell line	**Company**
Caco-2 cells	Sigma-Aldrich Corporation (St. Louis, Missouri, USA)
HCEC-1CT cells	UT Southwestern Medical Center (Dallas, Texas, USA)
THP-1 Lucia™ monocytes	InvivoGen (San Diego, California, USA)

Table 2: Cell culture reagents

Cell culture reagent	**Company**	**Lot/Catalog-Nr.**
Corning™ Epidermal Growth Factor (EGF), Human Recombinant	Corning Inc. (Corning, New York, USA)	1231003
Cosmic calf serum™	Corning Inc. (Corning, New York, USA)	/
Dulbecco`s Modified Eagle Medium (DMEM) [+] 4.5 g/l D-Glucose, L-Glutamine (500 ml)	Thermo Fisher Scientific Inc. (Waltham, Massachusetts, USA)	2786860
Dulbecco`s Modified Eagle Medium (DMEM) [+] 4.5 g/l D-Glucose, L-Glutamine, 25 mM HEPES (500 ml)	Thermo Fisher Scientific Inc. (Waltham, Massachusetts, USA)	2773589
Fetal Bovine Serum (FBS)	Thermo Fisher Scientific Inc. (Waltham, Massachusetts, USA)	2546614

Gentamicin	Life Technologies Corporation (Carlsbad, California, USA)	2873085
HEPES Buffer Solution (1M)	Thermo Fisher Scientific Inc. (Waltham, Massachusetts, USA)	2579412
Hydrocortisone (water soluble)	Sigma-Aldrich Corporation (St. Louis, Missouri, USA)	0000335190
Insulin-Transferrase-Selenium	Life Technologies Corporation (Carlsbad, California, USA)	2506883
Medium 199 (10x)	Thermo Fisher Scientific Inc. (Waltham, Massachusetts, USA)	2887791
Normocin 500 mg (10 x 1 ml)	InvivoGen (San Diego, California, USA)	NOL-46-02
Penicillin/Streptomycin (P/S) solution (10 000 Units/ml Penicillin, 10 000 µg/ml Streptomycin)	Life Technologies Corporation (Carlsbad, California, USA)	2585640
Roswell Park Memorial Institute 1640 medium (RPMI 1640) 500 ml	Thermo Fisher Scientific Inc. (Waltham, Massachusetts, USA)	2773770
Sodium Pyruvate 100 mM	Thermo Fisher Scientific Inc. (Waltham, Massachusetts, USA)	780661
Zeocin	InvivoGen (San Diego, California, USA)	ZEL-45-01

3.2. Test substances

Table 3: *Alternaria* mycotoxins (test substances)

Mycotoxin	**Supplier**	**Lot/ Charge Nr.**
ALT	Cayman Chemical (Ann Arbor, Michigan, USA)	0701458
ALTP	Cfm Oskar Tropitzsch (Marktredwitz, Germany)	/
AME	Synthesis Prof. Süßmuth TU Berlin (Berlin, Germany)	/
AOH	Szabo-Scandic (Vienna, Austria)	0695083-2
AST	Molport (Riga, Latvia)	NP-005288
ATX-I	Cayman Chemical (Ann Arbor, Michigan, USA)	0701456-1
TEN	Cayman Chemical (Ann Arbor, Michigan, USA)	0701460

3.3. Chemicals

Table 4: Chemicals

Chemical	**Company**	**Lot/ Charge Nr./ Cat.no.**
2-Mercaptoethanol	Carl Roth GmbH & Co. KG (Karlsruhe, Germany)	073196734
Accutase	Merck (Darmstadt, Germany)	3918977
CTB Reagent	Sigma-Aldrich Corporation (St. Louis, Missouri, USA)	0000514510
Dexamethasone (Dex)	Sigma-Aldrich Corporation (St. Louis, Missouri, USA)	/
Dimethylsulfoxide (DMSO)	Carl Roth GmbH & Co. KG (Karlsruhe, Germany)	Art.-Nr. A994.1
Ethylenediaminetetraacetic acid (EDTA)	Carl Roth GmbH & Co. KG (Karlsruhe, Germany)	123322105

Ethanol 96 %	Brenntag Austria GmbH (Vienna, Austria)	W241021
GAPDH primer, forward	Eurofins Genomics (Ebersberg, Germany)	S706Q4
GAPDH primer, reverse	Eurofins Genomics (Ebersberg, Germany)	S706Q4
High-Capacity cDNA Reverse Transcription Kit (1000 Reactions)	Thermo Fisher Scientific Inc. (Waltham, Massachusetts, USA)	2972013
Hs_CXCL8_1_SG	Qiagen (Hilden, Germany)	QT00000322
Hs_IL10_1_SG	Qiagen (Hilden, Germany)	QT00041685
Hs_IL6_1_SG	Qiagen (Hilden, Germany)	QT00083720
Hs_TNF_1_SG	Qiagen (Hilden, Germany)	QT00029162
KCl	Carl Roth GmbH & Co. KG (Karlsruhe, Germany)	475286543
KH_2HPO_4	Carl Roth GmbH & Co. KG (Karlsruhe, Germany)	38908471
Limulus Amebocyte Lysate (LAL) water	InvivoGen (San Diego, California, USA)	LAL-45-05
LPS from *E. coli*	Sigma-Aldrich Corporation (St. Louis, Missouri, USA)	/
Na_2HPO_2	Carl Roth GmbH & Co. KG (Karlsruhe, Germany)	020289971
NaCl	Carl Roth GmbH & Co. KG (Karlsruhe, Germany)	3902829120
PMA ≥ 99 %	Sigma-Aldrich Corporation (St. Louis, Missouri, USA)	/
Power SYBR™ Green PCR Master Mix	Thermo Fisher Scientific Inc. (Waltham, Massachusetts, USA)	2401651
QUANTI Luc™ 4 Lucia/Gaussia reagent	InvivoGen (San Diego, California, USA)	10668-4502
QUANTI Luc™ stabilizer	InvivoGen (San Diego, California, USA)	QLS-43-01

Recombinant human IL-1β	InvivoGen (San Diego, California, USA)	6409-45-02
Rotiphorese 50x TAE-buffer	Carl Roth GmbH & Co. KG (Karlsruhe, Germany)	Art.-Nr. CL86.1
Triton™ X-100	Carl Roth GmbH & Co. KG (Karlsruhe, Germany)	270298309
Trypan blue	Carl Roth GmbH & Co. KG (Karlsruhe, Germany)	/
Trypsin	Carl Roth GmbH & Co. KG (Karlsruhe, Germany)	1755489

3.4. Instruments

Table 5:Instruments

Instrument	**Specification**	**Company**
Autoclave	Systec DX-150	Systec GmbH (Linden, Germany)
Cell culture laminar	Herasafe KS	Thermo Fisher Scientific Inc. (Waltham, Massachusetts, USA)
Centrifuge	Hettich Zentrifugen Mikro 200	Andreas Hettich GmbH & Co. KG (Tuttlingen, Germany)
Centrifuge	Z 326 K	Hermle AG (Gosheim, Germany)
Freezer	Temperature: -20°C	Liebherr (Bulle, Switzerland)
Freezer	Temperature: -80°C	PHC Corporation (Tokyo, Japan)
Fridge	Temperature: 4°C	Liebherr (Bulle, Switzerland)
Ice machine	Scotsman MF 36	Scotsman Ice Systems (Vernon Hills, Illinois, USA)
Incubator	Heracell 240i	Thermo Fisher Scientific Inc. (Waltham, Massachusetts, USA)

Microplate reader	BioTec Synergy H1	BioTek Instruments, Inc. (Winooski, Vermont, USA)
Microscope	Axiocam 208 color	Carl Zeiss AG (Oberkochen, Germany)
Multichannel pipettes	Eppendorf Research plus (10-100 µl)	Eppendorf Research (Hamburg, Germany)
NanoDrop	NanoDrop 2000c Spectrophotometer	Thermo Fisher Scientific Inc. (Waltham, Massachusetts, USA)
PCR device	QuantStudio 3	Thermo Fisher Scientific Inc. (Waltham, Massachusetts, USA)
PCR Laminar	Peqlab	Peqlab Biotechnologie GmbH (Erlangen, Germany)
Pipettes	2.5 µl, 10 µl, 20 µl, 100 µl, 200 µl, 1000 µl, 5000 µl	Eppendorf GmbH (Hamburg, Germany)
Plate shaker	Vortemp 56	Labnet International, Inc. (Edison, New Jersey, USA)
Thermal cycler	C1000 Touch Thermal Cycler	Bio-Rad Labaratories, Inc. (Hercules, California, USA)
Vortexer	Vortexer-Genie 2	Scientific Industries (Bohemia, New York, USA)
Water bath	Grant GD100	Grant instruments (Cambridge, United Kingdom)

3.5. Consumables

Table 6: Consumables

Consumable	Specification	Company
Cell culture cultivation plate	Green 96-well Red 96-well Red 24-well Yellow 12-well Yellow 96-well	Sarstedt AG & Co. KG (Nümbrecht, Germany)
Cell culture flask	Green T175 Red T175 Yellow T175	Sarstedt AG & Co. KG (Nümbrecht, Germany)
Cover glass	24 x 24 mm	VWR International (Radnor, Pennsylvania, USA)
ELISA plate	96-well, black; white	Sarstedt AG & Co. KG (Nümbrecht, Germany)
Falcon tubes	13 ml, 15 ml, 50 ml	Sarstedt AG & Co. KG (Nümbrecht, Germany)
Filter tips	2.5 µl, 20 µl, 100 µl, 200 µl, 1000 µl	Sarstedt AG & Co. KG (Nümbrecht, Germany)
Gloves	Nitrile, powder free, blue	Th. Geyer GmbH & Co. KG (Renningen, Germany)
Micro tube	SafeSeal micro tube 2 ml	Sarstedt AG & Co. KG (Nümbrecht, Germany)
MicroAmp® Fast 96-Well Reaction Plate (0.1 ml)	PCR Compatible DNA/ RNA/ RNase Free	Thermo Fisher Scientific Inc. (Waltham, Massachusetts, USA)
MicroAmp™ Optical Adhesive Film	PCR/ Real-time PCR Compatible	Thermo Fisher Scientific Inc. (Waltham, Massachusetts, USA)
Needles	Yellow: Henke-Ject	Henke-Sass, Wolf (Tuttlingen, Germany)
Neubauer counting chamber	Depth: 0.1 mm; 0.0025 mm^2	Paul Marienfeld GmbH & Co. KG (Lauda-Königshofen, Germany)

Pasteur pipette	Lime-soda clear glass, total L 150 mm	Carl Roth GmbH & Co. KG (Karlsruhe, Germany)
Pipette tips	10 µl, 200 µl, 1000 µl, 5 ml	Sarstedt AG & Co. KG (Nümbrecht, Germany)
Precision wipes	11.2 x 12.3	Kimberly-Clark Professional (Roswell, Georgia, USA)
RNeasy Mini Kit (250)	178036984	Qiagen (Hilden, Germany)
Serological pipette	Volume: 5 ml, 10 ml	Sarstedt AG & Co. KG (Nürmbrecht, Germany)
Single-use syringe	Henke-Ject U-100 Insulin (1 ml)	Henke-Sass, Wolf (Tuttlingen, Germany)
Solution basin	55 ml, white	Biologix Europe GmbH (Hallbergmoos, Germany)
Tubes, 0.2 ml, domed cap	Certified DNA/ RNase free	Thermo Fisher Scientific Inc. (Waltham, Massachusetts, USA)

3.6. Software

Table 7:Software

Software	**Version**	**Company**
ChemSketch	Freeware Version 2022 2.3	Advanced Chemistry Development, Inc. (Toronto, Canada)
Exel	2501	Microsoft (Redmond, Washington, USA)
Gen5	3.08	BioTek Instruments, Inc. (Winooski, Vermont, USA)
NanoDrop	2000c	Thermo Fisher Scientific Inc. (Waltham, Massachusetts, USA)
Origin	OriginPro 2025b	OriginLab Corporation (Northampton, Massachusetts, USA)
QuantStudio Real Time PCR Software	QuantStudio™ Design & Analysis Software v1.5.1	Thermo Fisher Scientific Inc. (Waltham, Massachusetts, USA)
Word	2501	Microsoft (Redmond, Washington, USA)

3.7. Reagents and buffer

In the following the instructions for the preparation of the used buffers and solutions are reported.

3.7.1. Phosphate buffered saline

Table 8: Chemicals for preparation of phosphate buffered saline (PBS)

Chemical	**Amount [g]**	**Molarity [mM]**
KCl	2.54	34
KH_2PO_4	2.45	18
Na_2HPO_4	14.20	100
NaCl	100.00	17100

10 x PBS

- Salts were weighed and dissolved with 1 l distilled water
- pH was adjusted to 7.4
- sterile filtation
- Solution was stored at 4°C until further use

1 x PBS

- 1:10 dilution of 10 x PBS with distilled water
- autoclaved
- Solution was stored at 4°C until further use

3.7.2. Trypsin

Table 9: Chemicals for preparation of trypsin

Chemical	**Amount [mg]**
EDTA	250
Trypsin	500

Chemicals were dissolved in approximately 900 ml of autoclaved water and 100 ml of 10x PBS was added. pH was adjusted to 7.0 -7.4 and sterile filtration was performed. The solution was aliquoted and stored at -20°C.

4 Methods

This chapter describes the experimental design, procedures, and analytical approaches employed to achieve the objectives of the study.

4.1. Cell culture

When discussing the culture of mammalian cells, cells are initially isolated from tissues and subsequently maintained under controlled *in vitro* conditions. In order for the cells to survive in such conditions, it is crucial to closely mimic their natural environment, allowing them to proliferate and perform their specific functions. Key parameters such as temperature, pH, buffering capacity, as well as the presence of growth factors, hormones, and nutrients, play a critical role in successful cultivation. Therefore, specially formulated culture media are employed, providing most of these factors and representing an optimal combination for supporting cell growth under *in vitro* conditions [56].

4.1.1. Cultivation of THP-1 Lucia™ monocytes

THP-1 is a human monocytic cell line isolated from the peripheral blood of a child diagnosed with acute monocytic leukemia (subtype M5). It is widely recognized as a relevant *in vitro* model for studying monocyte structure and function under both physiological and pathological conditions. THP-1 cells have a round, non-adherent morphology, and expresses recognizable monocytic markers. Its main characteristic is unlimited proliferation and resistance to apoptosis, which is a result of its neoplastic (leukemic) origin. It is often used due to its ability to mimic the differentiation process into macrophages and its similarity to primary monocytes and macrophages in terms of morphology and biological responses [39,57]. Cells were maintained in culture medium (RPMI 1640) supplemented with 10 % heat-inactivated FBS, 1 % P/S, 25 mM HEPES buffer and 100 µg/ml normocin. Cells were sub-cultured every third to fourth day (see Figure 3). They were grown in a humified atmosphere at 37°C and 5 % CO_2 in green T-175 flasks. Cells were counted as described in chapter 4.2, and the volume of cell suspension required to obtain 9×10^6 cells was calculated accordingly. Fresh cultivation medium was added to reach a total volume of 30 ml. To maintain selection pressure and thereby ensure the stability of the reporter gene, 100 µg/ml of zeocin is added to the growth medium every other passage.

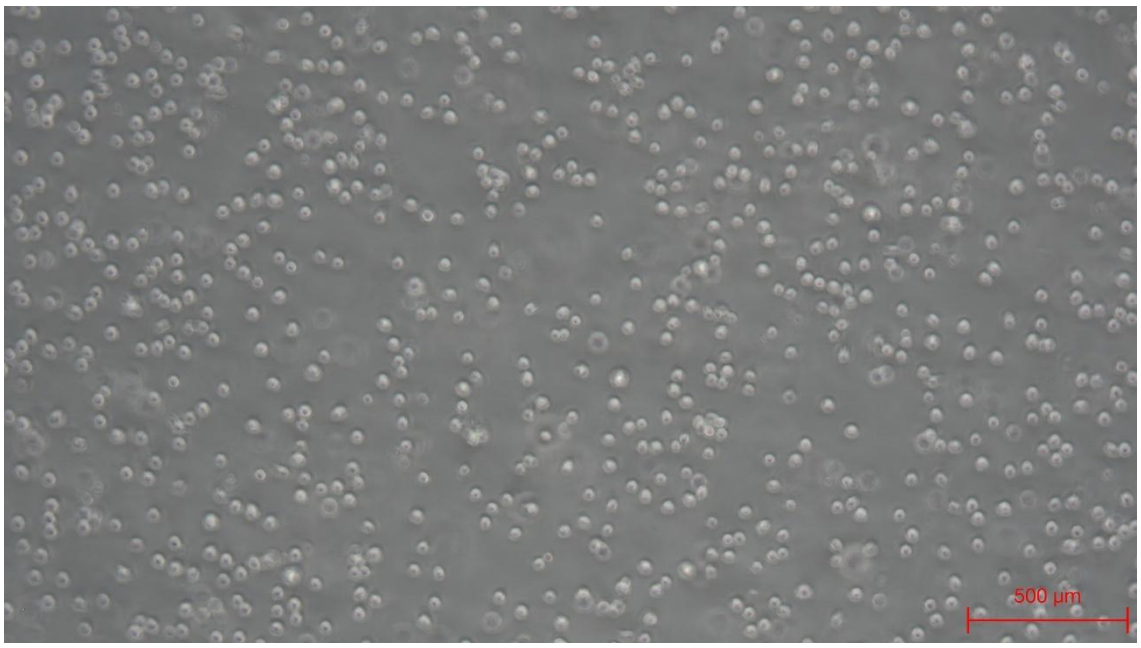

Figure 3: THP-1 Lucia™ monocytes under the microscope after 4 days of cultivation; scale bar: 500 µm

4.1.2. Cultivation of Caco-2 cells

The Caco-2 cell line originates from a human colon adenocarcinoma and is unique due to its ability to undergo differentiation upon reaching full confluence. Differentiated Caco-2 cells exhibit various morphological and functional characteristics typical for small intestinal enterocytes [40]. They form a monolayer, have a cylindrical and polarized shape, possess microvilli on the apical surface, and are connected by tight junctions. In addition, they express enzyme activities specific to the apical membrane of enterocytes [58]. Caco-2 cells were cultivated in DMEM supplemented with 10 % heat-inactivated FBS, 1 % P/S, 1 mM sodium pyruvate and 0.01 mg/ml insulin-transferrin-selenium. Cells were sub-cultured every third to fourth day at 70-80 % of confluence (see Figure 4) and grown in a humified atmosphere at 37°C and 5 % CO_2. Red T-175 flasks were used for cultivation. Cells were counted as described in chapter 4.2. For a growth period of three days, 2 x 10^6 cells were seeded in 28 ml culture medium, while for four days 1.5 x 10^6 cells were further cultivated. Only Caco-2 cells with a passage number below 20 were used for this study.

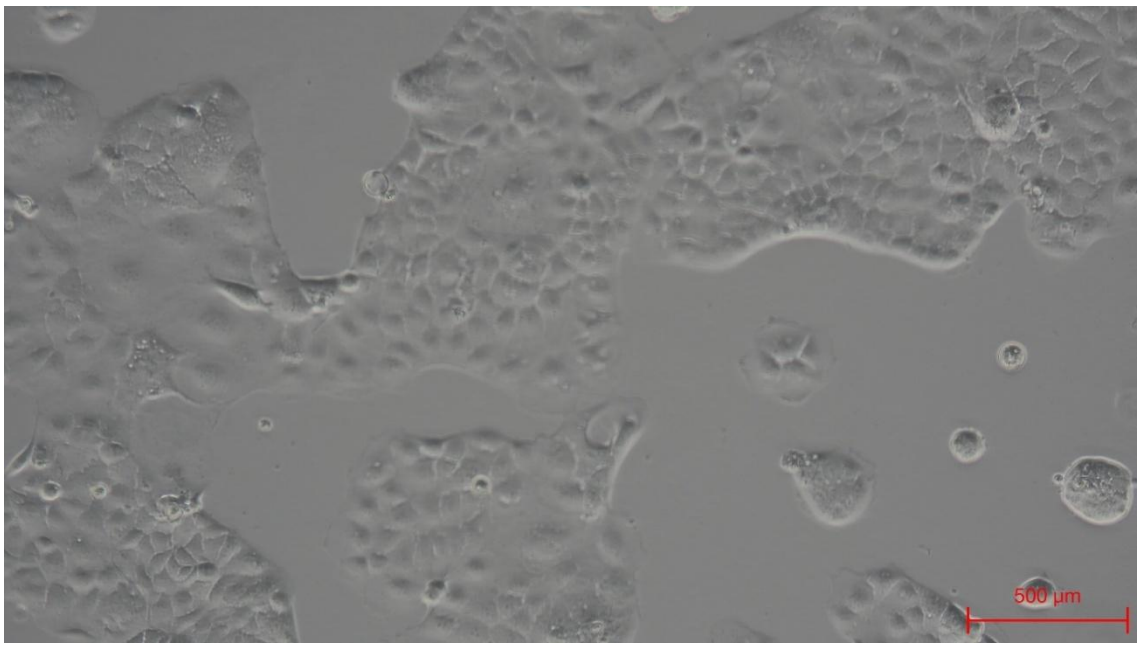

Figure 4: Caco-2 cells under the microscope after 3 days of cultivation; scale bar: 500 µm

4.1.3. Cultivation of HCEC-1CT cells

HCEC-1CT is an immortalized, non-cancerous human colonic epithelial cell line that serves as a representative model of the intestinal epithelium, the primary site of exposure to ingested substances [59]. Cells were incubated in DMEM supplemented with 2 %cosmic calf serum™, 2% Medium 199, 20 mM HEPES buffer, 50 µg/ml gentamicin, 1 µg/ml hydrocortisone, 10 µl/ml insulin-transferrin-selenium and 20 ng/ml recombinant human EGF. Cells were sub-cultured every third to fourth day at 70-80 % of confluence (see Figure 5) and incubated in humified atmosphere at 37°C and 5 % CO_2. Yellow T-175 flasks were used for cultivation. For splitting the cells, the growth medium was aspirated, and the cells were washed with 10 ml of PBS. Cells were incubated with 3.5 ml of accutase for 3 min. 10 ml of growth medium was added, and the suspension was transferred to a falcon tube. The cell count was determined as described in chapter 4.2. For a growth period of three days 0.9×10^6 cells and for four days 0.7×10^6 cells were seeded in 30 ml of growth medium respectively. Only HCEC-1CT cells with a passage number below 30 were used for this study.

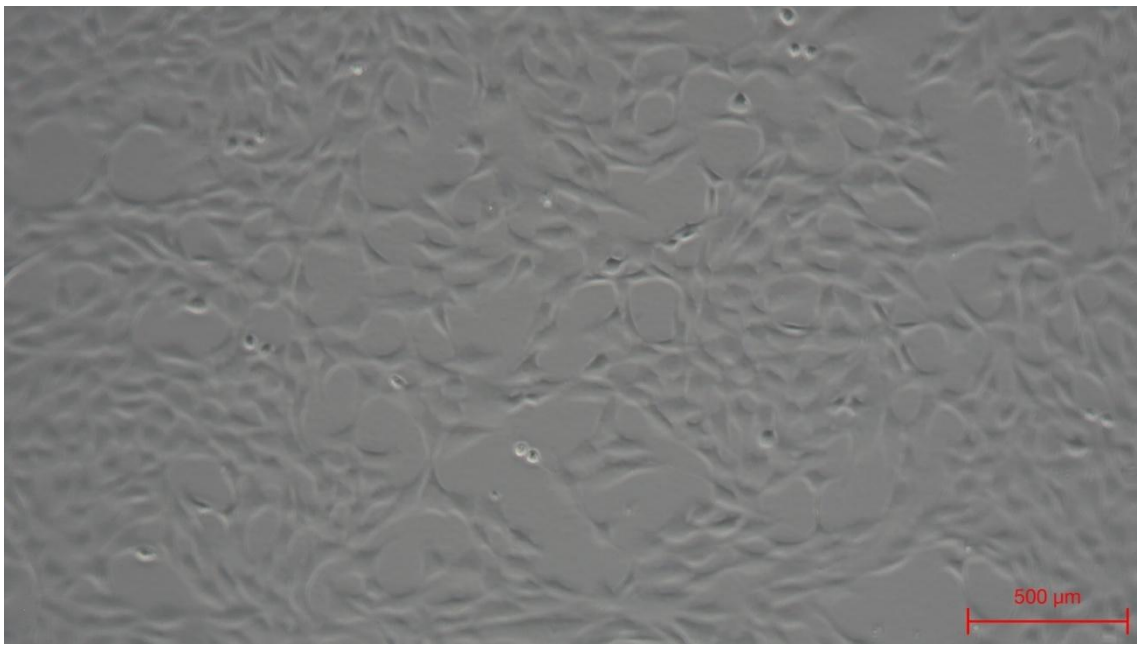

Figure 5: HCEC-1CT cells under the microscope after 4 days of cultivation; scale bar: 500 µm

4.2. Cell counting

To determine the cell number, cell suspension was diluted 1:5 with trypan blue and pipetted into the Neubauer counting chamber (see Figure 6). Trypan blue selectively stains non-viable cells, allowing the distinction between live (unstained) and dead (blue-stained) cells. Cells within 4 defined squares (consisting of 4x4 squares each) were counted under the microscope. Only unstained, viable cells were used for calculating cell concentration and two counting grits were evaluated.

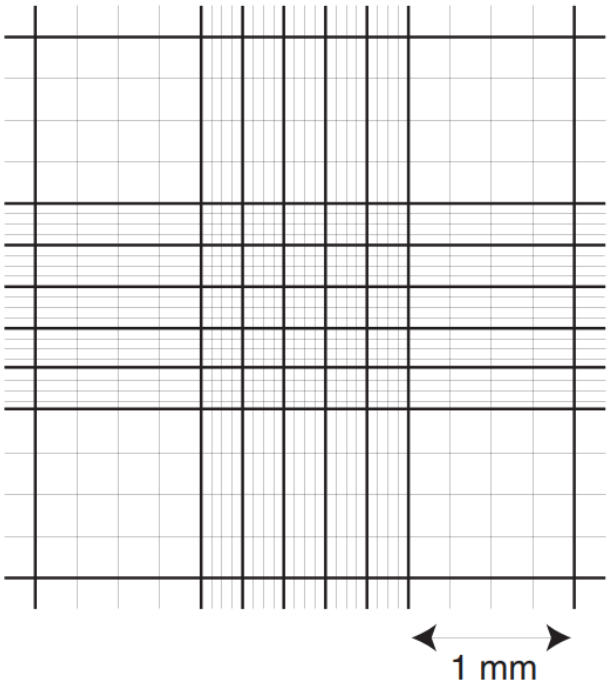

Figure 6: Schematic representation of Neubauer counting chamber [60]

After the viable cells were counted, the cell number per ml was determined using Equation 1. First, the average number of cells per large square was determined and then multiplied by the factor 10^4, which represents the volume factor of the Neubauer counting chamber, and finally multiplied by the dilution factor. In this way, the cell concentration in 1 ml is obtained.

$$\frac{Cells}{ml} = average\ cell\ number * 10^4 * dilution\ factor$$

Equation 1: Cell concentration per ml

4.3. NF-κB reporter gene assay

THP-1 Lucia™ monocytes are derived from the THP-1 monocyte cell line and have been genetically modified by stable integration of an NF-κB-inducible Lucia luciferase reporter construct. These cells are specifically designed to study the NF-κB signaling pathway. This modification allows precise monitoring of NF-κB activation by quantifying the activity of Lucia luciferase secreted into the cell culture supernatant. Detection of luciferase activity can be realized using the specialized, pre-formulated bioluminescent assay reagent, QUANTI Luc™ 4 Lucia/Gaussia [61,62].

4.3.1. Seeding and incubation of THP-1 Lucia™ monocytes

The NF-κB reporter gene assay with THP-1 Lucia™ monocytes was performed in green 96-well plates. The plate set-up was different for each measurement to avoid possible systematic errors. Each assay set-up contained solvent, positive and negative controls, as well as different concentrations of the tested mycotoxins. All test substances were dissolved and diluted in DMSO and stock solutions were prepared in a concentration 400 times higher than the test concentration. All solutions were diluted 1:200 with medium. For the solvent control and the positive control medium containing 0.5 % DMSO was used. For the latter cells were later additionally stimulated with 10 ng/ml LPS. As negative control served 1 µM Dex. In monocytes different concentrations of ALT and TEN (0.01-25 µM) were tested for their immunomodulatory properties. Per plate each control and test condition were tested in technical triplicates. For that, 100 µl of the test solutions were transferred to the respective wells. The required cell count was 1 x 10^5 cells/well. After counting the cells (see chapter 4.2), the required volume of cell suspension was transferred to a falcon tube and centrifuged at 140 rcf for 2 min. The medium was aspirated while the pellet was resuspended in fresh culture medium. The suspension was gently mixed and 100 µl were transferred to the wells of the 96-well plate that already contained 100 µl of test medium. Accordingly, final volume in the wells was 200 µl. The final DMSO concentration in all conditions was 0.25 %. The plate was shaken for 1 min at 50 rcf and incubated for 2 h at 37°C and 5 % CO_2. Afterwards, LPS was added to the positive and negative control as well as the wells containing

the mycotoxins. The 400 ng/ml LPS stock solution was prepared in medium without additives. The final concentration of LPS per well was 10 ng/ml. The plate was incubated for an additional 18 h.

4.3.2. Seeding and incubation of THP-1 Lucia™ macrophages

96 h prior to the incubation of the cells with the test compounds 1 x 10^5 monocytes per well were seeded in a red 96-well plate. After counting the cells (see chapter 4.2), the required volume of cell suspension was transferred to a falcon tube and centrifuged at 140 rcf for 2 min. The medium was gently aspirated, and the pellet was resuspended in fresh culture medium. For differentiation from monocytes to macrophages (see Figure 7) 10 ng/ml PMA was applied. The 10 µg/ml PMA stock solution was prepared in DMSO. Cells were incubated at 37°C and 5 % CO_2 for 72 h. At the end of incubation time, the PMA-containing medium was removed and the cells were exposed to with PMA-free growth medium for another 24 h. PMA is a strong activator of Protein Kinase C (PKC) [63] and is commonly used to induce activation and differentiation of THP-1 Lucia™ NF-κB monocytes into macrophage Like cells. Following incubation with PMA, the cells must be cultured in PMA-free growth medium to allow for recovery and stabilization prior to their use in subsequent assays [64].

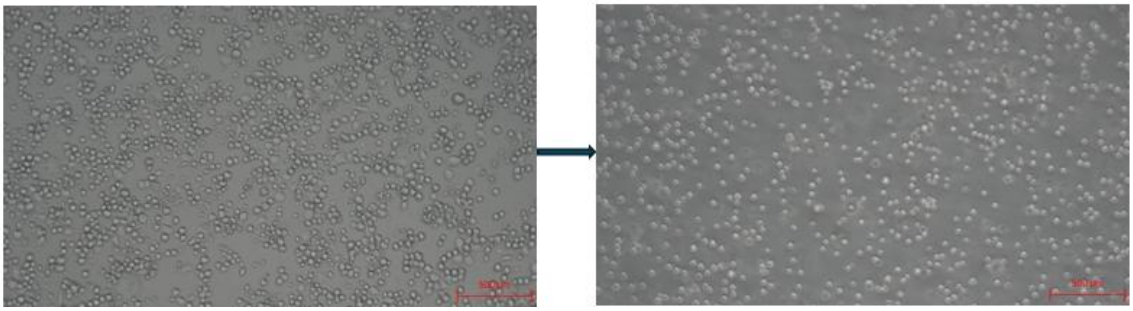

Figure 7: Differentiation of monocytes to macrophages; scale bar 500 µm

The preparation of test media and all subsequent experimental steps were performed as described for monocytes. (see chapter 4.3.1). Table 10 displays an overview of the *Alternaria* mycotoxins and respective concentrations tested.

Table 10: Concentrations of stock solutions and final concentrations of mycotoxins tested in THP-1 Lucia™ macrophages

Mycotoxin	**Final concentration [µM]**
ALT	0.01; 0.1; 1; 2; 5; 10; 25
ALTP	0.01; 0.1; 1; 2; 5; 10
AME	0.01; 0.1; 1; 2; 5; 10; 25
AOH	0.01; 0.1; 1; 2; 5; 10; 25
AST	0.01; 0.1; 1; 2; 5; 10; 25
ATX-I	0.01; 0.1; 1; 2; 5; 10; 25, 50
TEN	0.01; 0.1; 1; 2; 5; 10; 25

4.3.3. Detection of luciferase activity

After a total incubation time of 20 h, the plate was shaken for 1 min at 50 rcf and centrifuged at 140 rcf for 2 min. 20 µl of the cell suspension from each well were transferred to a white ELISA plate. As blank THP-1 medium was measured under the same conditions. In the dark, 50 µl of light-sensitive QUANTI Luc™ 4 reagent with stabilizer (prepared according to the manufacturer's instructions) was added to each well. The plate was gently tapped several times prior to measurement. Luminescence was measured using the plate reader (BioTec Synergy H1) and Gen 5 software.

4.4. CellTiter-Blue® Cell Viability Assay

The CTB assay is a simple, fluorometric method for measuring cellular metabolic activity which ultimately reflects cell viability. Viable cells can reduce the dye resazurin to resorufin, which changes the spectral characteristics of the reagent. Initially dark blue and minimally fluorescent, resazurin is metabolized to the pink, highly fluorescent resorufin with excitation and emission peaks at 579nm and 584 nm, respectively. Non-viable cells rapidly lose metabolic activity, fail to reduce resazurin, and therefore do not produce a fluorescent signal (see Figure 8) [65].

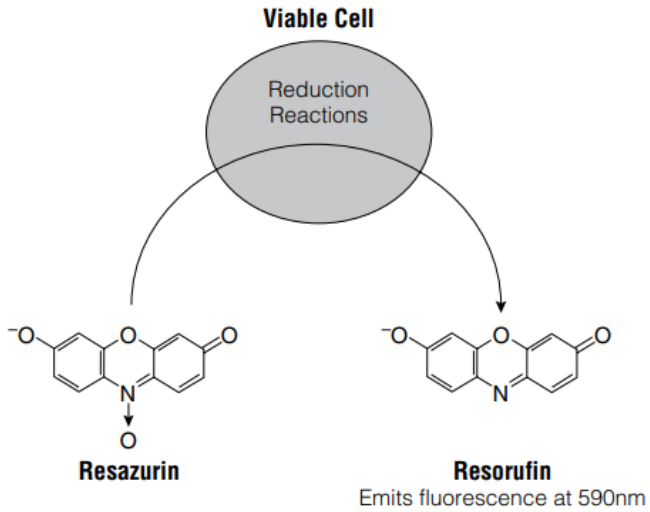

Figure 8: Reduction of resazurin to resorufin by metabolically active cells. The formation of the fluorescent product is proportional to cellular metabolic activity [65]

4.4.1. CTB assay in THP-1 Lucia™ monocytes and macrophages

To ensure that the results of the NF-κB reporter gene assay are not only artefacted caused by cytotoxicity, the CTB assay was always carried out in parallel in the same plate used for the NF-κB reporter gene assay (see chapters 4.3.1, 4.3.2 and 4.3.3) and after detection of luciferase activity. Triton™ X-100 was used as a positive control for cytotoxicity and was added to 3 wells containing only medium and cells. The Triton™ X-100 solution was prepared in growth medium, and the final concentration was 0.01 %. In the dark, 20 µl of light-sensitive CTB reagent was added to each well. The plate was shaken for 1 min at 50 rcf and incubated for 2 h at 37°C and 5 % CO_2. At the end of incubation time, the plate was shaken again, centrifuged at 140 rcf for 2 min and 100 µl from each well were transferred to a black 96-well ELISA plate. Measurements were performed with a plate reader equipped with the Gen 5 software and fluorescence was measured at 590 nm and excitation at 560 nm.

4.4.2. CTB assay in Caco-2 cells

The CTB assay in Caco-2 cells was performed before qRT-PCR experiments to determine if the *Alternaria* mycotoxins of interest exert cytotoxicity. Therefore, only concentrations that showed no cytotoxic effects on the both selected cell lines (Caco-2 and HCEC-1CT), were used for PCR measurements, ensuring the reliability of the results. Cells were seeded in red 96-well plates and a cell number of 24,650 cells/well in 100 µl growth medium was applied. Cells were cultivated for 7 days at 37°C and 5 % CO_2 to obtain a tight and partially differentiated Caco-2 cell monolayer (see **Error! Reference source not found.**). The culture medium was changed three times during d ifferentiation.

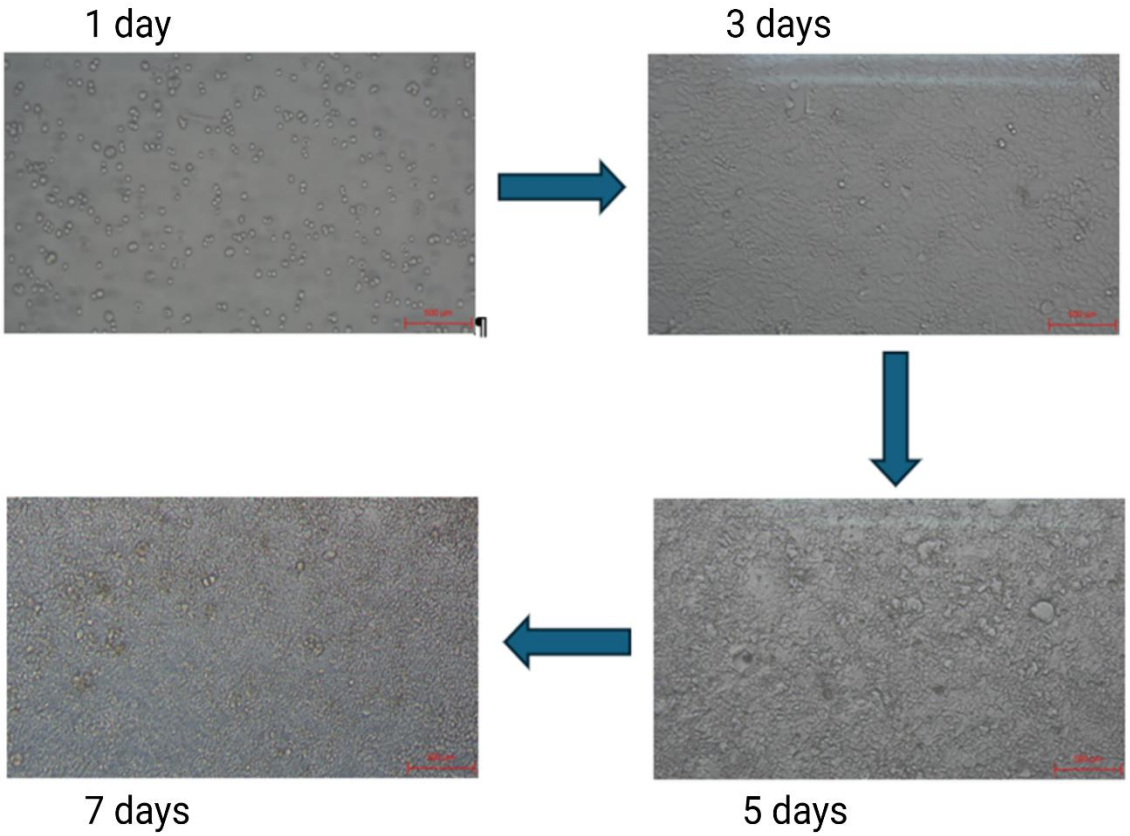

Figure 9: Differentiation of Caco-2 cells during cultivation for 7 days (after 1, 3, 5 and 7 days) at 37°C and 5 % CO_2 until a partially differentiated Caco-2 cell monolayer is created; scale bar 500 µm.

As indicated in Table 11, different concentrations of the seven *Alternaria* mycotoxins were examined for possible cytotoxic properties. The mycotoxin stock solutions were prepared in DMSO and diluted 1:100 with growth medium. As solvent control 1 % DMSO and as negative control 1 µM Dex were used respectively.

Table 11: Final concentrations of mycotoxins tested in Caco-2 cells for CTB measurement.

Mycotoxin	**Final concentration [µM]**
ALT	0.1; 1; 10; 25; 50; 100
ALTP	0.01; 0.1; 1; 5; 10; 25; 50
AME	0.1; 1; 10; 25; 50; 100
AOH	0.1; 1; 10; 25; 50; 100
AST	0.1; 1; 10; 25; 50; 100
ATX-I	1; 10; 25, 50; 100; 200
TEN	0.1; 1; 10; 25; 50; 100

Cell medium was replaced with 100 µl of the test solutions The plate was incubated for 2 h at 37°C and 5 % CO_2. After 2 h of incubation, cells were additionally exposed to 25 ng/ml IL-1β for further 18 h. 5 µl of a 500 ng/ml IL-1β solution in medium without additives was added to all wells except those containing medium control and solvent control. For the positive control cells were incubated with 1 % DMSO for 2 h followed by the addition of IL-1β. After a total incubation of 20 h, the cell culture medium was removed, and the cells were washed with a prewarmed PBS solution. PBS was replaced with 100 µl of CTB solution (1:10 dilution with transparent DMEM medium without additives) in the dark. As blank Caco-2 medium without cells was used. For positive cytotoxicity control, a 0.1 % Triton™ X-100 solution in DMEM was applied. The plate was incubated for 2 h at 37°C and 5 % CO_2. After incubation, 80 µl of the supernatant was transferred to a black 96-well plate and fluorescence was measured using a plate reader and Gen 5 software.

4.4.3. CTB assay in HCEC-1CT cells

To assess possible effects of the test substances on the viability of HCEC-1CT cells, 5000 cells/well in 100 µl growth medium were seeded into yellow 96-well plates. Cells were grown for 48 h at 37°C and 5 % CO_2 to obtain a confluent monolayer (see Figure 10).

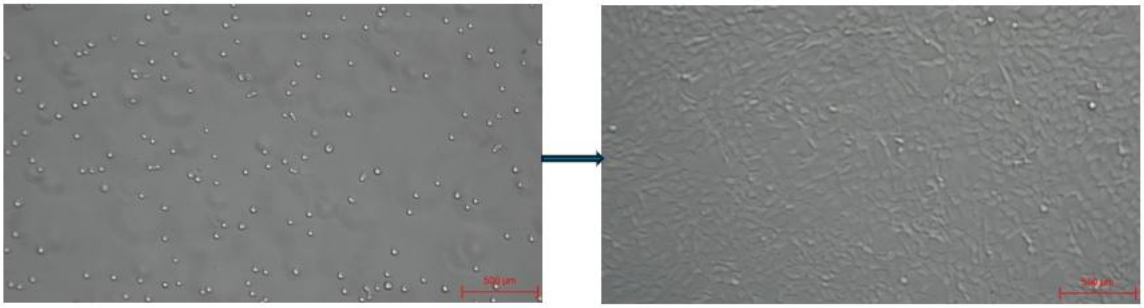

Figure 10: HCEC-1CT cells after incubation for 48 h; scale bar 500 µm

The experimental procedure of the CTB assay was analogous as described for Caco-2 cells (see chapter 4.4.2). As blank HCEC-1CT medium without cells was used. The concentrations of tested mycotoxins are indicated in Table 12.

Table 12: Final concentrations of mycotoxins tested in HCEC-1CT cells for CTB measurement

Mycotoxin	**Final concentration [µM]**
ALT	0.01; 0.1; 1; 10; 25; 50; 100
ALTP	0.001; 0.01; 0.1; 1; 2.5; 5; 10; 25; 50
AME	0.01; 0.1; 1; 10; 25; 50; 100
AOH	0.01; 0.1; 1; 10; 25; 50; 100
AST	0.01; 0.1; 1; 10; 25; 50; 100
ATX-I	0.1; 1; 10; 25, 50; 100; 200
TEN	0.01; 0.1; 1; 10; 25; 50; 100

4.5. Quantitative real-time polymerase chain reaction

qRT-PCR analysis was used to determine the mRNA transcript levels of various pro-and anti-inflammatory cytokines such as IL-6, IL-8, IL-10, and TNF-α, in order to investigate the potential immunomodulatory effects of mycotoxins on the non-immune cell lines Caco-2 and HCEC-1CT. The principle of PCR is based on the denaturation of double-stranded DNA. Specific oligonucleotide molecules (primer) bind (annealing) to the 5' and 3' ends of the region to be amplified. These oligonucleotides are extended (elongation) by a DNA polymerase in the presence of free deoxynucleoside triphosphates (dNTPs). The polymerase continues to elongate the newly formed DNA double strand until it either dissociates from the DNA or the reaction is interrupted. Such an interruption can occur, for example, by raising the incubation temperature to 95 °C, which causes repeated denaturation of the double-stranded DNA. Cooling the reaction mixture to a range of 60-40 °C in the presence of free oligonucleotides allows them to bind to complementary sequences of the DNA template based on their melting temperature (Tm). At this stage, the synthesis of another double strand can be initiated. After 25-30 cycles, quantification of the amplified PCR products becomes increasingly difficult. To enable quantification of target amplicons, optical PCR systems have been developed to monitor the amplification process in real time. This approach, RT-PCR allows the amount of amplified DNA to be measured directly. Fluorescent molecules (fluorophores), typically attached to sequence-specific oligonucleotides, are commonly used as detection tools in RT-PCR. Small molecules can intercalate between double-stranded nucleic acids and emit longer wavelength light (530 nm) when excited by short-wavelength UV light. The intercalator SYBR Green™ has proven effective for the specific detection of double-stranded DNA (dsDNA). Fluorescence intensity increases in proportion to the amount of

amplified DNA. The PCR program is tailored to the RT-PCR parameters or the requirements of the specific PCR system [66].

4.5.1. Cell cultivation, test media preparation and incubation of Caco-2 and HCEC-1CT cells

The following section describes the cultivation of Caco-2 and HCEC-1CT cells, the preparation of test media, and the incubation of cells for qRT-PCR analysis.

4.5.1.1. Test media preparation and incubation of Caco-2 cells

Incubation of Caco-2 cells with the different mycotoxins for qRT-PCR measurement was performed in red 24-well plates and 155,000 cells/well in 1000 µl growth medium were seeded. Cell cultivation and proliferation was carried out in the same way as for the CTB assay (see chapter 4.4.2). All test solutions were diluted 1:1000 with growth medium. As solvent control 0.1 % DMSO and as negative 1 µM Dex were used respectively. Different, non-cytotoxic concentrations of *Alternaria* mycotoxins were tested, as indicated in the Table 13.

Table 13: Final concentrations of *Alternaria* mycotoxins tested in Caco-2 cells with qRT-PCR.

Mycotoxin	**Final concentration [µM]**
ALT	0.1; 0.5; 1; 5; 10
ALTP	0.1; 1; 2.5; 5; 10
AME	0.1; 1; 10
AOH	0.1; 1; 10; 30
AST	0.1; 1; 10
ATX-I	0.1; 1; 10; 20
TEN	0.01; 0.1; 1; 10

After a proliferation time of 7 days, the growth medium was replaced with 500 µl of test solution. The plate was incubated for 2 h at 37 °C and 5 % CO_2. After 2 h of incubation, 10 µl of a 1.25 µg/ml IL-1β solution in medium without additives was added to all wells except those containing medium control and solvent control. For the positive control cells were incubated with 0.1 % DMSO for 2 h followed by the addition of IL-1β. For all stimulated conditions the final concentration of IL-1β was 25 ng/ml. The plate was further incubated for an additional 3 h at 37 °C and 5 % CO_2. After a total incubation of 5 h, cell lysis was performed.

4.5.1.2. Test media preparation and incubation of HCEC-1CT cells

Incubation of HCEC-1CT cells with the different test substances for qRT-PCR measurement was performed in yellow 12-transwell plates and 63,000 cells/ well in 2000 µl growth medium was seeded. Cell cultivation was carried out in the same way as described for the CTB assay (see chapter 4.4.3). The preparation of test solutions and controls, as well as the incubation of HCEC-1CT cells, were performed in the same way as for Caco-2 cells (see chapter 4.5.1.1). The final concentrations of tested, non-cytotoxic *Alternaria* mycotoxins on HCECE-1CT cells are indicated in Table 14.

Table 14: Final concentrations of *Alternaria* mycotoxins tested in HCEC-1CT cells with qRT-PCR

Mycotoxin	**Final concentration [µM]**
ALT	0.1; 1; 5; 10
ALTP	0.1; 1; 2.5
AME	0.1; 1; 10
AOH	0.1; 1; 10; 30
AST	0.1; 1; 10
ATX-I	0.1; 1; 10; 20
TEN	0.1; 1; 10

4.5.2. qRT-PCR

The following qRT-PCR protocol was applied to both Caco-2 and HCEC-1CT cell lines.

4.5.2.1. Cell lysis

Cell medium was collected in Eppendorf tubes for further experiments. Cells were washed with cold PBS and 350 µl of RLT Lysis buffer containing 1 % β-Mercaptoethanol were added to each well. Using a pipette tip, the cells were detached from the bottom of the wells. The cell solutions were pipetted up and down several times, transferred to Eppendorf tubes, and further lysed multiple times using disposable syringes and yellow needles. Cell lysated were stored at -80°C.

4.5.2.2. RNA extraction

The RNeasy Mini Kit was used for total RNA extraction, following manufacturer's instructions. First, samples were thawed, and one volume of 70 % ethanol (340 µl) was added. Samples were transferred to a spin column and centrifuged at 9180 rcf for 1 min. Flow through was discarded and 700 µl of RW1 buffer was added to each spin column. Tubes were centrifuged at 9180 rcf for 1 min and the flow-through was discarded. In the next step, 500 µl of RPE buffer was added, centrifuged at the same program and the flow through discarded. Another 500 µl of RPE buffer were added but tubes were centrifuged at 15 000 rcf for 3 min. Spin columns were transferred to a new collection tube and centrifuged at 15 000 rcf for 3 min. Spin columns were then transferred to an elution tube and 30 µl of RNAse-free water was added to each spin column. The columns were centrifuged at 9180 rcf for 1 min. For higher RNA yields, the flow-through was again pipetted onto the spin column, centrifuged at 9180 rcf for 1 min and immediately placed on ice. The RNA concentration of the samples was determined using a NanoDrop 2000c spectrophotometer. RNAse-free water was used as a blank.

4.5.2.3. Reverse Transcription

After RNA extraction and determination of RNA concentration, total RNA was reverse transcribed into complementary DNA (cDNA). All steps were performed on ice. Samples were diluted with RNAse water to obtain a final concentration of 1000 ng RNA.
A reverse transcription master mix was prepared using the High Capacity cDNA Reverse Transcription Kit. In total it was prepared for of n + 2 samples. In the following the reagents and respective volumes required for one sample (n = 1) are listed:

- 2 µl 10x RT buffer
- 0.8 µl dNTP

- 2 µl random primers
- 1 µl RT
- 4.2 µl H_2O

The master mix was added to each sample in a ratio 1:2 and solutions were mixed by snipping. The samples were placed in a thermo cycler and the program used for reverse transcription was set as indicated in Table 15. Samples were stored at -20°C until further use.

Table 15: Temperature und time settings for reverse transcription

Settings	**Step 1**	**Step 2**	**Step 3**	**Step 4**
Temperature	25°C	37°C	85°C	4°C
Time	10 min	120 min	5 min	Hold

4.5.2.4. qRT-PCR measurement

Samples were diluted with RNAse free water to obtain a final cDNA concentration of 10 ng/µl. GAPDH was used as a housekeeping gene. Possible changes in transcript levels of IL-6, IL-8, IL-10 and TNF-α using commercially available primer assays. The respective master mixes for each gene were prepared for n + 2 samples. In the following the reagents and respective volumes required for one sample (n = 1) are listed:

- 6 µl RNAse free water per well
- 2 µl primer per well (or 1 µl each in case of separate forward and reverse primer)
- 10 µl SYBR Green per well

18 µl of the PCR-master mix were pipetted into a 96-well PCR plate and 2 µl of diluted cDNA was added to the wells to obtain a final cDNA concentration of1 ng/µl.
As a negative control RNAse free water was used. The plate was then sealed with a transparent adhesive foil and centrifuged at 140 rcf for 2 min. The following PCR program using the Step One software was used:

- Initial phase: 15 min at 95°C
- Cycling stage: 40 cycles: 15 s at 94°C, 30 s at 55°C, 30 s at 72°C
- Melt curve stage: 1 min at 65°C; heating in 0.5°C steps to 94°C, 15 s at 95°C,
- Baseline setting: cycle 3 to 15

The $2^{-\Delta\Delta C_T}$ method was applied to calculate relative changes in gene transcription [67]. The obtained threshold cycle (C_T) values of the target genes (IL-6, IL-8, IL-10, TNF-α) were normalized to the average C_T value of the housekeeping gene GAPDH (ΔC_T of sample) and then compared to the

corresponding positive control (ΔC_T of 25 ng/ml IL-1 β). In this way, the $\Delta\Delta C_T$ value was obtained (see Equation 2). Afterwards, the $2^{-\Delta\Delta C_T}$ value was calculated (see **Error! Reference source not found.**), and the results were presented as mean ± standard deviation (SD).

$$\Delta\Delta C_T = \Delta C_T \; of \; sample - \; \Delta C_T \; of \; IL - 1ß$$

Equation 2: $\Delta\Delta C_T$ value

$$\text{Relative mRNA transcript level} = 2^{-\Delta\Delta C_T}$$

Equation 3: Relative mRNA transcript level

4.5.3. Data evaluation

All measurements were conducted with at least three technical and three biological replicates. For data evaluation, mean values + SD was calculated from a minimum of three biological replicates. All measurements were normalized to the respective positive control except for CTB measurements for THP-1 Lucia™ monocytes, which were normalized to the respective solvent control (0.25 % DMSO). As a positive control for THP-1 Lucia™ monocytes and macrophages 10 ng/ml LPS, whereas for Caco-2 and HCEC-1CT cells 25 ng/ml IL-1β was used. To determine statistically significant differences between the samples and the respective positive control, an independent Student's *t*-test was applied. This test was also used to determine statistically significant differences between the same concentrations of a given mycotoxin in Caco-2 and HCEC-1CT cell lines for results of CTB measurements. Samples showing significant differences compared to the control or between cell lines were marked (* $p < 0.05$; ** $p < 0.01$; *** $p < 0.001$). One-way analysis of variance (ANOVA) followed by Fisher LSD post-hoc test was used to determine statistically significant differences between the different concentrations of one given mycotoxin. Significant differences between the tested concentrations are indicated by different letters above the bars for $p < 0.05$. All statistical analyses and graphs generation were performed using OriginPro 2025b software.

5 Results

In the following section, the results of the conducted experiments are presented.

5.1. Immunosuppressive and cytotoxic effects of *Alternaria* mycotoxins in THP-1 Lucia™ monocytes and macrophages

To investigate the potential immunosuppressive and cytotoxic effects of selected *Alternaria* mycotoxins, the NF-κB reporter gene assay and the CTB assay were conducted in THP-1 Lucia™ monocytes and macrophages. Results obtained from both cell types can be compared and can potentially lead to a better understanding of the immunosuppressive activity of the mycotoxins under investigation.

5.1.1. Immunosuppressive and cytotoxic effects of *Alternaria* mycotoxins in THP-1 Lucia™ monocytes

In THP-1 Lucia™ monocytes, immunosuppressive effects of ALT and TEN were evaluated using NF-κB reporter gene assay. Both mycotoxins were tested at concentrations ranging from 0.01 to 25 µM and the respective results are depicted in Figure 11. Compared to the positive control (10 ng/ml LPS), both TEN and ALT exhibited moderate immunosuppressive properties (Figure 11a). TEN induced a concentration-dependent reduction in NF-κB activity, with statistically significant effects observed from 2 µM onwards, where the signal decreased to 80.1 ± 11.2% ($p < 0.05$). For ALT, a clear concentration-dependent decrease started at 5 µM with a signal of 73.7 ± 8.6% ($p < 0.05$). At the highest tested concentration of 25 µM, TEN and ALT reduced the signal to 51.4 ± 16.6% ($p < 0.001$) and 63.9 ± 9.6% ($p < 0.001$), respectively. Additionally, to be able to exclude experimental artefacts associated with cytotoxicity, the CTB assay was carried out. Accordingly, neither ALT nor TEN showed cytotoxic effects at the tested concentrations in THP-1 Lucia™ monocytes (Figure 11b).

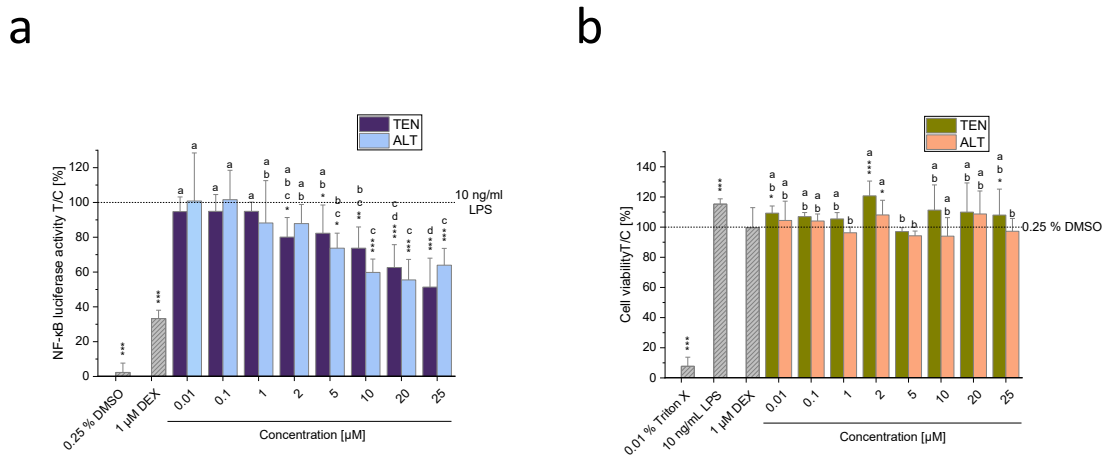

Figure 11: Effects of ALT and TEN on the NF-κB signaling activity and cell viability of THP-1 Lucia™ monocytes under simultaneous lipopolysaccharide (LPS) stimulation. (a) shows the results of the NF-κB assay, while (b) displays the results of the CTB assay, which was performed in parallel. All data are expressed as mean + SD of at least three biological replicates and were normalized to the positive control (10 ng/ml LPS) for the NF-κB assay and the solvent control (0.25 % DMSO) for the CTB assay. 1 µM dexamethasone (DEX) served as a negative control for the NF-κB assay (a), while 0.01 % Triton™ X-100 was used as a cytotoxicity control for the CTB assay (b). Statistical significance compared to the positive control (a), or the solvent control (b) was determined by Student's *t*-test (* $p < 0.05$; ** $p < 0.01$; *** $p < 0.001$). One-way ANOVA followed by Fisher's LSD post hoc test was applied to determine statistically significant differences between the different concentrations of each mycotoxin (a-d; $p < 0.05$).

5.1.2. Immunosuppressive and cytotoxic effects of *Alternaria* mycotoxins in THP-1 Lucia™ macrophages

In THP-1 Lucia™ macrophages, immunosuppressive effects were evaluated for all seven *Alternaria* mycotoxins (AOH, AME, ALT, ALTP, ATX-I, TEN and AST). The three dibenzo-α-pyrones AOH, AME, and ALT were tested at concentrations ranging from 0.01 to 25 µM (Figure 12a). AOH induced a concentration-dependent suppression of LPS-induced NF-κB activation with significant inhibition starting at 1 µM and a reduction to 55.0 ± 12.8% ($p < 0.001$). AME also exerted a concentration-dependent effect and significantly reduced NF-κB luciferase activity already at the lowest tested concentration of 0.01 µM, resulting in 74.7 ± 21.2% activity ($p < 0.01$). In contrast to AOH and AME, ALT exhibited weaker immunosuppressive effects. At a concentration of 5 µM, a slight suppression of NF-κB activity was observed with a signal reduction to 65.8 ± 14.5% ($p < 0.001$). At the highest tested concentration of 25 µM, AOH and AME showed similar results, with a signal reduction to 26.2 ± 16.5% ($p < 0.001$). and 21.4 ± 10.5% ($p < 0.001$), respectively, while for ALT the signal was reduced to 64.3 ± 16.4% ($p < 0.001$).

The impact of AOH, AME and ALT on cell viability was assessed in parallel (Figure 12b). AOH showed mild cytotoxicity at 1 µM, with cell viability reduced to 86.3 ± 9.6% ($p < 0.01$), while at the highest tested concentration cell viability dropped to 64.6 ± 10.9% ($p < 0.001$). Incubation of

macrophages with AME resulted in a concentration-dependent decrease in cell viability, with a reduction already apparent at 0.1 µM (76.4 ± 6.2%; $p < 0.001$). At the highest tested concentration, cell viability dropped further to 44.3 ± 2.0% ($p < 0.001$). In contrast, ALT did not exhibit cytotoxicity at any of the tested concentrations.

Possible immunosuppressive effects of the perylene quinones ALTP and ATX-I, as well as the *Alternaria* mycotoxins TEN and AST were also investigated (Figure 12c). TEN significantly suppressed NF-κB activity at 5 µM with a signal reduction to 73.8 ± 18.2% ($p < 0.01$). For AST, significant suppression ($p < 0.001$) started at 0.1 µM, with a signal reduction to 57.0 ± 5.5%. At a concentration of 25 µM, TEN showed a suppression of LPS-induced NF-κB activation to 66.3 ± 11.5% ($p < 0.001$) and AST to 58.6 ± 22.0% ($p < 0.001$). Among all tested compounds, ALTP was the *Alternaria* mycotoxin with the strongest immunosuppressive effect. It significantly suppressed LPS-induced NF-κB activation already at 1 µM, reducing the signal to 14.7 ± 9.8% ($p < 0.001$). In contrast, ATX-I only showed slight immunosuppressive activity starting at a concentration of 5 µM (67.1 ± 11.8%; $p < 0.05$). However, a significant suppression was observed at 25 µM, with NF-κB luciferase activity reduced to 28.6 ± 14.3% ($p < 0.001$). At the highest tested concentration of 20 µM, ALTP reduced NF-κB signaling to 2.5 ± 0.004% ($p < 0.001$), whereas ATX-I, at the highest tested concentration of 50 µM, reduced the signal to 8.2 ± 4.6% ($p < 0.001$).

As shown in Figure 12d, TEN did not exhibit cytotoxicity at any of the tested concentrations. In contrast, both AST and ATX-I caused a significant reduction in cell viability at 25 µM. For AST, cell viability was reduced to 72.9 ± 8.4% ($p < 0.001$), and for ATX-I to 81.6 ± 20.6% ($p < 0.05$). ALTP also showed cytotoxic effects at the highest tested concentration of 20 µM, with a signal reduction to 44.8 ± 11.4% ($p < 0.001$).

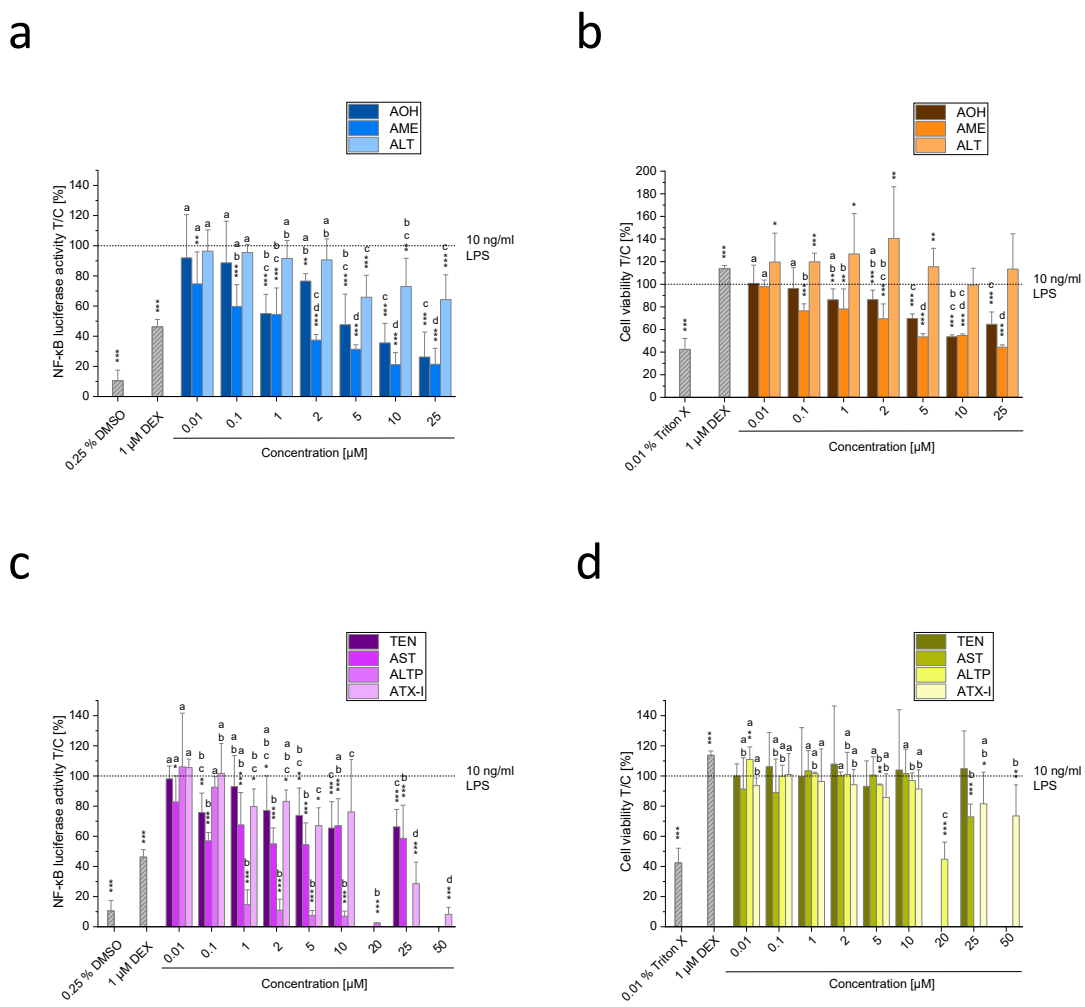

Figure 12: Effects of the seven *Alternaria* mycotoxins (AOH, AME, ALT, TEN, AST, ALTP, ATX-I) on the NF-κB signaling activity and cell viability of THP-1 Lucia™ macrophages under simultaneous lipopolysaccharide (LPS) stimulation. (a) and (c) show the results of the NF-κB assay, while (b) and (d) display the results of the CTB assay, which was performed in parallel. All data are expressed as mean + SD of at least three biological replicates and were normalized to the positive control (10 ng/ml LPS). 1 µM dexamethasone (DEX) served as a negative control for the NF-κB assay (a) and (c), while 0.01 % Triton™ X-100 was used as a cytotoxicity control for the CTB assay (b) and (d). In graphs where a specific bar is missing for a certain concentration of the tested mycotoxin, those concentrations were not measured. Statistical significance compared to the positive control was determined by Student's *t*-test (* $p < 0.05$; ** $p < 0.01$; *** $p < 0.001$). One-way ANOVA followed by Fisher's LSD post hoc test was applied to determine statistically significant differences between the different concentrations of each mycotoxin (a-d; $p < 0.05$).

5.2. Cytotoxic and immunosuppressive effects of *Alternaria* mycotoxins on the intestinal epithelial cell lines Caco-2 and HCEC-1CT

The following section presents the results of cytotoxic and immunosuppressive effects of the seven *Alternaria* mycotoxins on the intestinal epithelial cell lines Caco-2 and HCEC-1CT. The possible cytotoxic properties of mycotoxins were investigated using the CTB assay, while potential immunosuppressive effects were examined through qRT-PCR. To avoid misinterpretation of gene expression data, only non-cytotoxic concentrations-as determined by the CTB assay- were used for subsequent qRT-PCR analyses. Relative mRNA expression levels of selected pro-and anti-inflammatory cytokines (IL-6, IL-8, IL-10, and TNF-α) were measured and cells were additionally stimulated with IL-1β (25 ng/ml) to induce a proinflammatory state.

5.2.1. Cytotoxic effects of *Alternaria* mycotoxins on Caco-2 and HCEC-1CT cells

For the elucidation of possible cytotoxic effects different concentrations of the selected *Alternaria* mycotoxins were tested in Caco-2 and HCEC-1CT cells. The respective results are depicted in Figure 13.

Cell viability after AOH (Figure 13a) treatment was assessed at concentrations ranging from 0.01 to 100 µM (Figure 13b). Only the highest tested concentration (100 µM) showed a slight but statistically significant decrease in metabolic activity in both cell lines (Caco-2: 78.7 ± 5.4%; HCEC-1CT: 74.1 ± 13.6%; $p < 0.001$). The results between the two cell lines did not differ significantly, except at the concentration of 0.1 µM, where a minor difference was observed ($p < 0.05$). Furthermore, AME (Figure 13c) was not found to be cytotoxic in Caco-2 cells. However, in HCEC-1CT cells, a decrease in cell viability began at a concentration of 5 µM where the signal decreased to 77.8 ± 10.8% ($p < 0.01$). At the highest tested concentration of 100 µM, the signal dropped to 26.9 ± 8.9% ($p < 0.001$; Figure 13d). The results between the two cell lines differed significantly only at the four highest tested concentrations (10 and 25 µM - $p < 0.05$; 50 µM and 100 µM - $p < 0.001$). In contrast, the dibenzo-α-pyrone ALT (Figure 13e) did not exhibit cytotoxicity in neither Caco-2 nor HCEC-1CT cells within the tested concentration range from 0.01 to 100 µM (Figure 13f).

The perylene quinone ATX-I (Figure 13g) showed significantly more potency in HCEC-1CT cells than in Caco-2 cells (Figure 13h). It exerted only mild cytotoxicity in Caco-2 cells at the highest tested concentration of 200 µM (84.9 ± 11.8%) without statistically significant differences compared to the positive control, whereas in HCEC-1CT cells, a decrease in cell viability began at 50 µM (75.4 ± 21.4%; $p < 0.01$). At the highest tested concentration, cell viability was reduced

to 24.7 ± 13.8% ($p < 0.001$). The results between the two cell lines differed significantly for the two highest tested concentrations ($p < 0.001$). As for ALTP (Figure 13i) concentrations ranging from 0.001 to 50 µM were tested (Figure 13j). In Caco-2 cells, ALTP induced strong cytotoxic effects only at the highest tested concentration of 50 µM, with an almost complete loss of viable cells (1.1 ± 1.8%; $p < 0.001$). In contrast, in HCEC-1CT cells, ALTP demonstrated higher potency, with significant cytotoxicity already observed starting at a concentration of 5 µM (59.55 ± 11.9%; $p < 0.001$). Statistical analysis revealed that at concentrations ranging from 5 to 25 µM, the results obtained for both cell lines differed significantly ($p < 0.001$).

The *Alternaria* mycotoxins with miscellaneous structures, TEN (Figure 13k) and AST (Figure 13m), were also tested for their cytotoxic potential. TEN did not exert any cytotoxicity at the tested concentrations in neither Caco-2 nor HCEC-1CT cells (Figure 13l). On the other hand, AST was cytotoxic only in HCEC-1CT cells at the highest tested concentration of 100 µM (31.3 ± 14.3%; $p < 0.001$; Figure 13n). Significant differences between the two cell lines were observed only at certain concentrations. For TEN, differences exist for 0.1 µM ($p < 0.05$) and 10 µM ($p < 0.05$), while for AST for 0.1 µM ($p < 0.05$), 10 µM ($p < 0.05$), and 100 µM ($p < 0.001$).

a

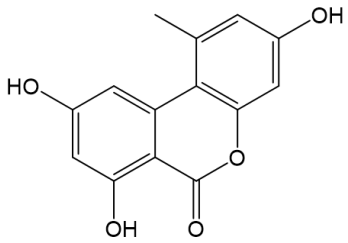
HO
OH
O
OH
O

b

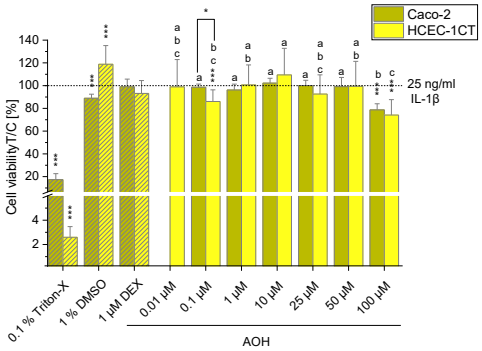
Caco-2
HCEC-1CT
Cell viability T/C [%]
25 ng/ml
IL-1β
0.1 % Triton-X
1 % DMSO
1 µM DEX
0.01 µM
0.1 µM
1 µM
10 µM
25 µM
50 µM
100 µM
AOH

c

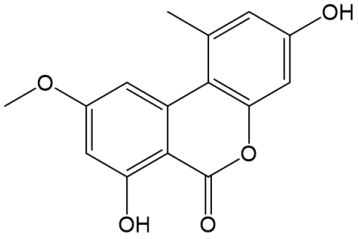
OH
O
O
OH
O

d

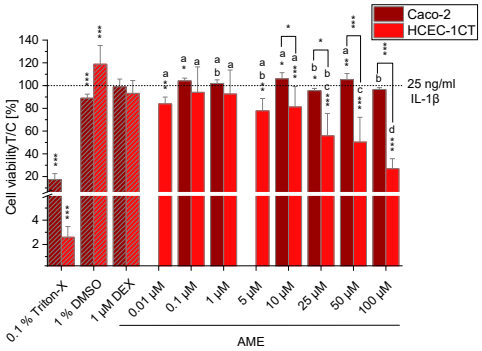
Caco-2
HCEC-1CT
Cell viability T/C [%]
25 ng/ml
IL-1β
0.1 % Triton-X
1 % DMSO
1 µM DEX
0.01 µM
0.1 µM
1 µM
5 µM
10 µM
25 µM
50 µM
100 µM
AME

e

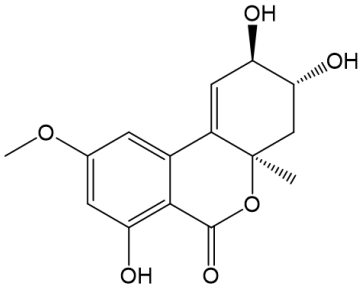
OH
OH
O
O
OH
O

f

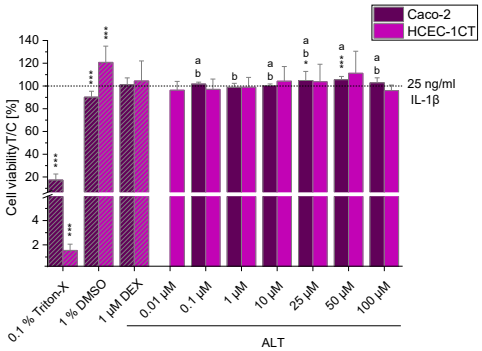
Caco-2
HCEC-1CT
Cell viability T/C [%]
25 ng/ml
IL-1β
0.1 % Triton-X
1 % DMSO
1 µM DEX
0.01 µM
0.1 µM
1 µM
10 µM
25 µM
50 µM
100 µM
ALT

g

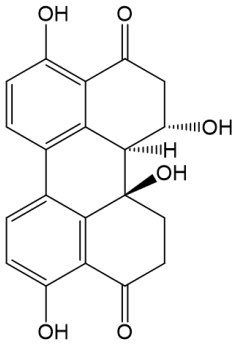
OH
O
OH
H
OH
OH
O

h

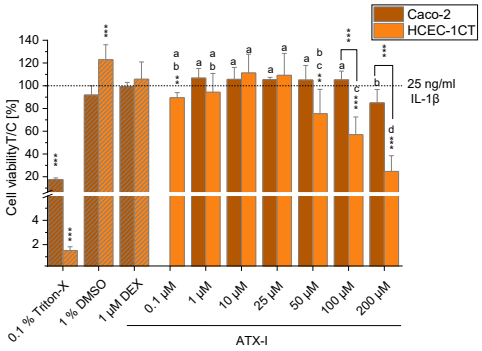
Caco-2
HCEC-1CT
Cell viability T/C [%]
25 ng/ml
IL-1β
0.1 % Triton-X
1 % DMSO
1 µM DEX
0.1 µM
1 µM
10 µM
25 µM
50 µM
100 µM
200 µM
ATX-I

i

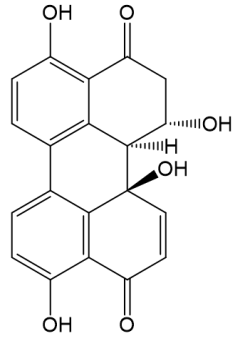
OH
O
OH
H
OH
OH
O

j

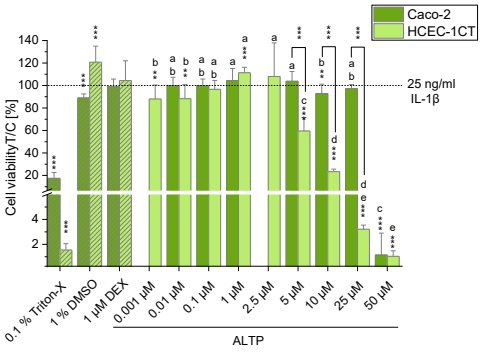
Caco-2
HCEC-1CT
Cell viability T/C [%]
25 ng/ml
IL-1β
0.1 % Triton-X
1 % DMSO
1 µM DEX
0.001 µM
0.01 µM
0.1 µM
1 µM
2.5 µM
5 µM
10 µM
25 µM
50 µM
ALTP

k

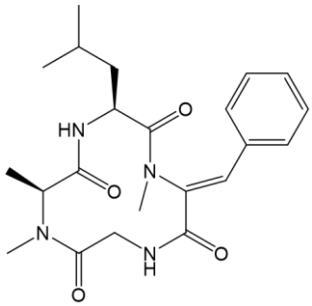
HN
O
N
O
N
H
O
O

l

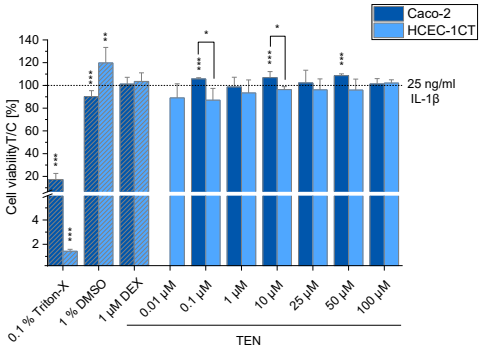
Caco-2
HCEC-1CT
Cell viability T/C [%]
25 ng/ml
IL-1β
0.1 % Triton-X
1 % DMSO
1 µM DEX
0.01 µM
0.1 µM
1 µM
10 µM
25 µM
50 µM
100 µM
TEN

m

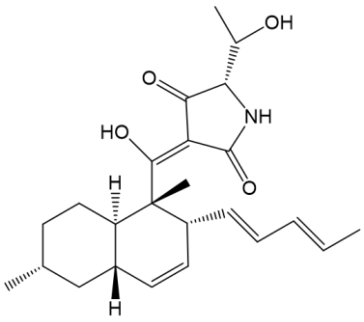

n

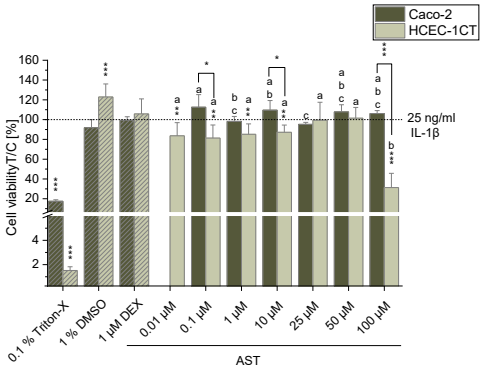

Figure 13: Impact of *Alternaria* mycotoxins AOH (a), AME (c), ALT (e), ATX-I (g), ALTP (i) TEN (k), and AST (m) on cell viability (b, d, f, h, j, l, n) in interleukin 1β (IL-1β) stimulated Caco-2 and HCEC-1CT cells, measured with CTB assay. Cells were pre-incubated with toxins or 1 µM dexamethasone (DEX) for 2 h, followed by stimulation with IL-1β (25 ng/ml) for further 18 h. All data are expressed as mean + SD of at least three biological replicates and were normalized to the positive control (25 ng/ml IL-1β). 0.1 % Triton X™-100 served as a control for cytotoxicity. Student's *t*-test was used to determine statistically significant differences compared to the positive control, as well as between the same concentration of one toxin tested in Caco-2 and HCEC-1CT cells (* $p < 0.05$; ** $p < 0.01$; *** $p < 0.001$). One-way ANOVA followed by Fisher's LSD post hoc test was applied to determine statistically significant differences between the different concentrations of each mycotoxin (a-e; $p < 0.05$).

5.2.2. Immunosuppressive effects of ALTP and AOH on Caco-2 and HCEC-1CT cells

The two *Alternaria* mycotoxins that had a significant impact on changes in the transcription of genes of the tested pro-and anti-inflammatory cytokines in non-immune cells Caco-2 and HCEC-1CT were ALTP (see chapter 0) and AOH (see chapter 5.2.2.2).To evaluate changes in gene transcription, fold change thresholds are commonly applied. A gene is considered upregulated if its expression increases at least twofold (fold change ≥ 2), and downregulated if expression is reduced by half or more (fold change ≤ 0.5). These thresholds indicate significant alterations in gene expression levels [68]. Accordingly, all other tested toxins exhibited no immunosuppressive effects. They respective data are presented in Supplementary results.

5.2.2.1. Immunosuppressive effects of ALTP on Caco-2 and HCEC-1CT cells

In Caco-2 cells, ALTP was tested at concentrations ranging from 0.1 to 10 µM, while in HCEC-1CT cells the tested range was 0.1 to 2.5 µM. These concentrations were selected based on the CTB assay results, which showed that within this range ALTP did not exhibit cytotoxicity in Caco-2 and HCEC-1CT cells (see Figure 13j). As shown in Figure 14a, ALTP reduced the transcription of IL-8 and TNF-α in Caco-2 cells starting at a concentration of 5 µM (IL 8: 0.132 ± 0.186, TNF-α:

0.4395 ± 0.254) and of IL-6 at a concentration of 10 µM (0.495 ± 0.148) with statistically significant decrease ($p < 0.001$). Changes in IL-6 transcription levels were statistically significant already at a concentration of 5 µM ($p < 0.001$), while for TNF-α at 1 µM ($p < 0.001$). However, the fold change was not ≤ 0.5 at these concentrations, meaning that the genes are not downregulated. Although IL-10 transcript levels showed a slight decrease, the reduction was statistically significant compared to the positive control only at the highest tested concentration of 10 µM ($p < 0.01$), but no downregulation occurred.

As depicted in Figure 14b, ALTP significantly reduced the expression of both pro-and anti-inflammatory cytokines in a concentration-dependent manner in HCEC-1CT cells. At a concentration of 1 µM, a statistically significant decrease was measured, particularly for IL-6 (0.067 ± 0.036; $p < 0.001$), IL-8 (0.31 ± 0.085; $p < 0.001$), and TNF-α (0.44 ± 0.23; $p < 0.001$). The strongest inhibitory effects were observed at 2.5 µM, where the transcription levels of all cytokines were markedly reduced. The reduction in IL-6 expression was more pronounced in HCEC-1CT cells (2.5 µM: 0.015 ± 0.006; $p < 0.001$) compared to Caco-2 cells (10 µM: 0.49 ± 0.15; $p < 0.001$).

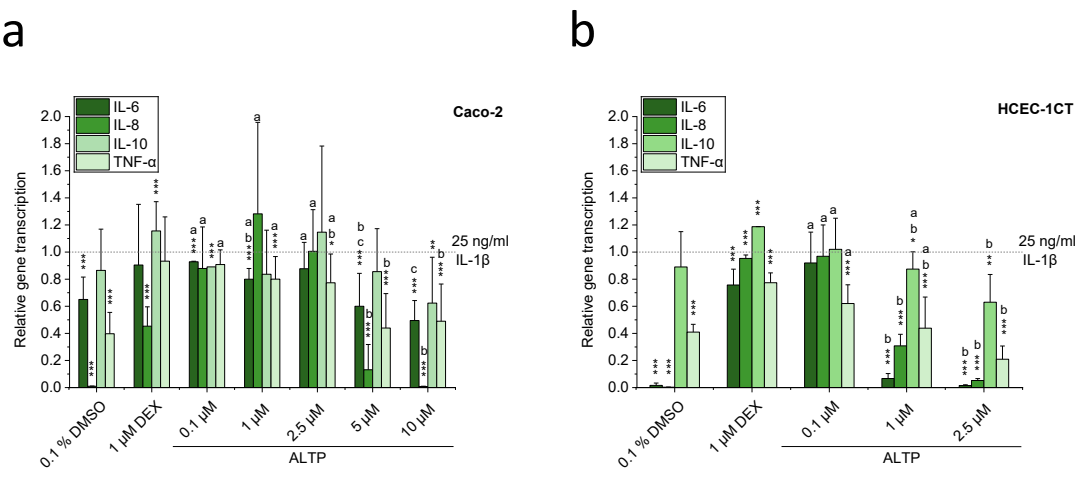

Figure 14: Impact of ALTP on relative gene transcription levels of IL-6, IL-8, IL-10 and TNF-α in interleukin 1β (IL-1β) stimulated Caco-2 (a) and HCEC-1CT (b) cells, measured with qRT-PCR. Cells were pre-incubated with ALTP or 1 µM dexamethasone (DEX) for 2 h, followed by stimulation with IL-1β (25 ng/ml) for further 3 h. Changes in gene transcript levels are shown as mean + SD of at least three biological replicates, calculated as relative gene transcription ($2^{-\Delta\Delta CT}$), normalized to GAPDH and compared to the positive control (25 ng/ml IL-1β). Student's *t*-test was used to determine statistically significant differences compared to the positive control (* $p < 0.05$; ** $p < 0.01$; *** $p < 0.001$). One-way ANOVA followed by Fisher's LSD post hoc test was applied to determine statistically significant differences between the different tested concentrations of ALTP (a-c; $p < 0.05$).

5.2.2.2. Immunosuppressive effects of AOH on Caco-2 and HCEC-1CT cells

Based on CTB results (see Figure 13b), relative gene transcription of AOH was analyzed in both cell lines at concentrations ranging from 0.1 to 30 µM. In Caco-2 cells, a slight increase in the expression of the pro-inflammatory cytokine TNF-α was observed at the highest tested concentration of 30 µM AOH, with a relative gene transcription of 1.45 ± 0.199 ($p < 0.001$; Figure 15a). Furthermore, in HCEC-1CT cells, IL-6 expression was reduced at 30 µM AOH to 0.505 ± 0.0278 although this change was not statistically significant. In contrast, TNF-α expression was significantly upregulated starting at a concentration of 10 µM ($p < 0.001$), with a relative gene transcription of 2.096 ± 0.0726 (Figure 15b).

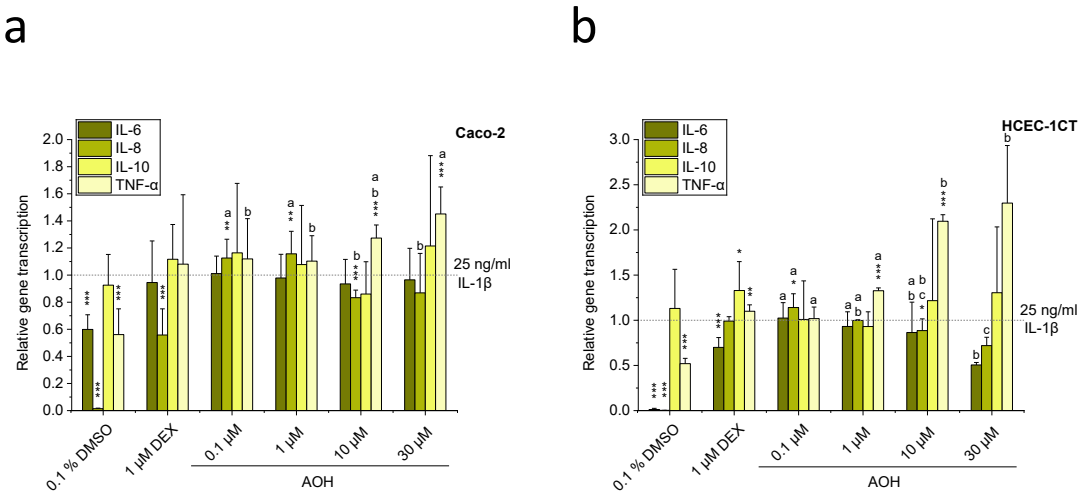

Figure 15: Impact of AOH on relative gene transcription levels of IL-6, IL-8, IL-10 and TNF-α in interleukin 1β (IL-1β) stimulated Caco-2 (a) and HCEC-1CT (b) cells, measured by qRT-PCR. Cells were pre-incubated with AOH or 1 µM dexamethasone (DEX) for 2 h, followed by stimulation with IL-1β (25 ng/ml) for further 3 h. Changes in gene transcript levels are shown as mean + SD of at least three biological replicates, calculated as relative gene transcription ($2^{-\Delta\Delta CT}$), normalized to GAPDH and compared to the positive control (25 ng/ml IL-1β). Student's t-test was used to determine statistically significant differences compared to the positive control (* $p < 0.05$; ** $p < 0.01$; *** $p < 0.001$). One-way ANOVA followed by Fisher's LSD post hoc test was applied to determine statistically significant differences between the different tested concentrations of AOH (a-c; $p < 0.05$).

6 Discussion

Fungi belonging to the genus *Alternaria* produce a wide array of mycotoxins which have been reported to exert different toxicological effects including cytotoxicity, genotoxicity, and detrimental effects on reproductive health [11–13]. However, information regarding their immunotoxic potential is still scarce. Therefore, in this study, the ability of individual *Alternaria* mycotoxins to target the NF-κB pathway, a central regulator of immune responses in immune cells, was investigated using THP-1 Lucia™ monocytes and PMA-differentiated macrophages [42]. This approach allowed the identification of mycotoxins with potential immunosuppressive properties. Beyond immune cells, IECs also play a crucial role in initiating innate immune responses and, due to their anatomical position, are directly exposed to high concentrations of ingested mycotoxins. Therefore, the effects of the different *Alternaria* toxins were additionally examined in the IEB using both cancer-derived Caco-2 cells and the non-cancerous HCEC-1CT line, in order to characterize their immunomodulatory properties in a physiologically relevant context.

Monocytes are generated in the bone marrow through the differentiation of monocyte/dendritic cell progenitors and primarily serve as precursors of macrophages. In addition, they play a role in immune surveillance, contribute to early inflammatory responses, and participate in tissue repair. In humans, monocytes are distinguished based on variations in the expression of CD14 and CD16 [69].Macrophages, on the other hand, arise from monocytes under specific conditions. In inflammatory states, circulating monocytes originating in the bone marrow infiltrate inflamed tissue and differentiate into macrophages. In addition, there is also a distinct population of tissue-resident macrophages that maintain homeostasis and have the capacity for self-renewal within tissues. Macrophages play a central role in host defense through phagocytosis of pathogens, clearance of dead cells, and regulation of inflammatory processes. Their remarkable phenotypic plasticity enables them to adapt to environmental signals and tissue-specific needs. Accordingly, they can polarize into two main functional subsets: M1 macrophages, which are pro-inflammatory and mediate pathogen defense and tissue damage, and M2 macrophages, which are anti-inflammatory and contribute to tissue repair and remodeling. This functional continuum (M1 ↔ M2) highlights their critical role in balancing immune responses [69].

In THP-1 Lucia™ macrophages, AOH induced a concentration-dependent suppression of LPS-induced NF-κB activation, with significant inhibition starting at 1 µM (see Figure 12a). Additionally, a reduction in cell viability was additionally observed at concentrations ≥ 1 µM (see Figure 12b). Although AOH was already cytotoxic at 1 µM, the reduction of NF-κB signal was around 45.0%, whereas the reduction in cell viability was only around 13.7%. The much stronger decrease in NF-κB activity compared to viability indicates a specific immunosuppressive effect that is

independent of cytotoxicity. These results are in accordance with previously published data, which have shown that AOH possesses immunosuppressive properties by inhibiting the activation of the NF-κB pathway in THP-1 macrophages [22], as well as in undifferentiated THP-1 Lucia™ monocytes starting at a concentration of 1 µM [29].

In addition to AOH, AME is one of the most extensively studied *Alternaria* mycotoxins. However, data regarding its immunosuppressive potential is still limited. Therefore, in the present study, AME was specifically investigated for its ability to suppress NF-κB activation in THP-1 Lucia™ macrophages (Figure 12a). At 0.01 µM, AME reduced NF-κB activity to 74.7% as compared to the LPS positive control (≈25% reduction), while cell viability remained unaffected, indicating a specific suppression of NF-κB independent of cytotoxicity. At 0.1 µM, cell viability decreased to 76.4% (≈24% reduction), showing that the suppression of NF-κB at higher concentrations is at least partly attributable to cytotoxic effects (Figure 12b). Previous studies have demonstrated that AME suppresses innate immune responses at a concentration of 10 µM in the BEAS-2B and RAW264.7 cells [24]. While these findings support the notion that AME exerts immunosuppressive effects, its role in modulating the LPS-induced NF-κB signaling pathway has not yet been fully elucidated. Given that BEAS-2B are human bronchial epithelial cells and RAW264.7 are murine monocyte-macrophage cells, they differ in origin from THP-1 Lucia™ monocytes and macrophages. Therefore, for future studies it would be useful to compare results obtained from cells of similar tissue and origin. This approach could provide deeper insights into the immunosuppressive effects of this mycotoxin and contribute to its potential regulation.

Alongside AOH and AME, ALT is classified within the dibenzo-α-pyrone group of mycotoxins; however, comprehensive data on its immunotoxicological properties are as of now not available, highlighting the need for further investigation into its potential impact on immune function. In the present study, ALT was evaluated for its effects in both THP-1 Lucia™ monocytes and macrophages. ALT suppressed LPS-induced activation of the NF-κB pathway in a concentration-dependent manner in THP-1 Lucia™ monocytes and macrophages, with statistically significant effects observed starting at 5 µM, (Figure 11a, Figure 12a). Furthermore, ALT did not exhibit cytotoxic properties in either of the cell lines, leading to the conclusion that the reduction in cell viability was not the cause of the decreased NF-κB pathway activity (Figure 11b and Figure 12b). Although toxicological data on this mycotoxin is limited, this study provides a first step in characterizing ALT as an immunosuppressive compound, highlighting the need for future research with greater focus on this toxin. In comparison with AOH, the results indicate that both mycotoxins exert similar effects in monocytes and macrophages. A likely explanation lies in their structural similarity, as both belong to the dibenzo-α-pyrone class of *Alternaria* toxins [11], which may account for their comparable ability to suppress the NF-κB pathway. Notably, however,

AOH, AME, and ALT differ in their cytotoxic profiles, suggesting that additional, yet poorly understood, mechanisms contribute to their biological activity. In this regard, although the results clearly demonstrate suppression of the NF-κB signaling pathway, they do not provide insight into the specific mechanism underlying this effect. It is well established that the NF-κB pathway can be regulated at several levels: at the initiation stage, by blocking signal reception through interference with receptor-ligand interactions, thereby preventing activation of the signaling cascade; at the cytoplasmic level, by modulating factors involved in signal transduction, with IKK and IκB proteins being the main targets; and at the nuclear level, by preventing the translocation of the NF-κB complex into the nucleus or by inhibiting its binding to DNA, which directly affects the transcription of target genes [42]. In this regard, Groestlinger et al. (2022) demonstrated that AOH reduces the nuclear translocation of the NF-κB/p65 subunit, a key regulator of the inflammatory response, while simultaneously promoting the mobilization of the aryl hydrocarbon receptor (AhR). This may indicate that the interaction between these two signaling pathways potentially contributes to the immunosuppressive effects of AOH [50]. Controversially, a study published by Solhaug at al. (2016) demonstrated that AOH increases ROS levels in the murine macrophage cell line RAW 264.7 [70]. Since ROS are known inducers of the NF-κB signaling pathway, it was expected that exposure to AOH would lead to ROS-mediated activation of NF-κB. However, although AOH elevates ROS levels, it simultaneously exerts immunosuppressive effects by inhibiting NF-κB activity in LPS-stimulated THP-1 macrophages [22]. Based on these findings, it can be concluded that there is likely no direct link between AOH-induced ROS imbalance and the modulation of NF-κB activity. Additionally, it is important to note that AOH also reduces PMA-induced CD14 expression during the differentiation of monocytes into macrophages. Since CD14 is a key co-receptor of TLR4 in LPS-induced macrophage activation, its reduction may have a significant impact on the immune response. Accordingly, Solhaug et al. (2016) could show that the presence of AOH during PMA-induced differentiation led to decreased LPS-induced secretion of TNF-α. These results confirm that AOH acts as an inhibitor of differentiation and the NF-κB signaling pathway [71]. Ultimately, future research has to be conducted to elucidate the molecular mechanisms underlying the observed immunosuppressive effects.

In addition to dibenzo-α-pyrones, the perylene quinones ALTP and ATX-I were also evaluated for their immunosuppressive potential in THP-1 Lucia™ macrophages. ALTP significantly suppressed LPS-induced NF-κB activation starting from 1 µM, while cytotoxic effects were observed only at the highest concentration tested (20 µM). Contradictory, ATX-I exhibited only modest immunosuppressive activity, with effects detectable starting at 5 µM and induced a reduction in cell viability starting at 25 µM. Although a statistically significant reduction in cell viability was observed at the highest tested concentration of ALTP and the two highest concentrations of ATX-

I, no decrease in viability was detected at the lowest active concentrations, thereby confirming the immunosuppressive effects of ALTP and ATX-I. These two compounds were selected for investigation based on the findings of Crudo et al. (2024) who investigated the effects of a complex extract of *Alternaria* mycotoxins on NF-κB activity. Through toxicity-guided fractionation, it could be shown that the fractions showing the strongest suppression of the NF-κB pathway contained substantial amounts of ALTP and ATX-I. Subsequently, these two compounds were tested individually and were identified as novel immunosuppressive *Alternaria* mycotoxins in THP-1 Lucia™ monocytes. In detail, they acted in a concentration-dependent manner, with effects becoming evident at concentrations as low as 1 µM [29]. These findings are in line with the present results. In both cell lines, ALTP induced a suppression of approximately 90% of luciferase activity already at 1 µM, highlighting its high potency. Moreover, the extent of ATX-I-mediated suppression only slightly differed between the two cell types (monocytes, 10 µM: 52.8%; macrophages, 10 µM: 76.1%). Regarding the mechanisms of action of this group of *Alternaria* toxins, it has been shown that ATX-I, due to the absence of an epoxide group compared to ATX-II, does not induce lipid peroxidation or membrane alterations. In contrast, ATX-II, at subtoxic concentrations, reduces NF-κB activation but, unlike LPS, does not trigger nuclear translocation of the p65 subunit. Moreover, ATX-II induces lipid peroxidation, which, in combination with membrane cholesterol, leads to increased mitochondrial superoxide production, mitochondrial reorganization, and suppression of the NF-κB signaling pathway [44].

The third group of mycotoxins investigated comprised *Alternaria* mycotoxins with miscellaneous structures, among which TEN and AST were selected. In the present thesis, TEN was evaluated for immunosuppressive properties for the first time, being tested in both monocytes (Figure 11a) and macrophages (Figure 12c). In monocytes, TEN suppressed LPS-induced activation of the NF-κB pathway in a concentration-dependent manner starting at 2 µM, whereas in macrophages a reduction in signal was observed from 5 µM, with a comparable potency (monocytes: 2 µM, 80.1%; macrophages: 5 µM, 73.8%), leading to the conclusion that, like the other tested mycotoxins, it exhibits similar effects in both cell lines. Within the tested concentration range, TEN did not exhibit cytotoxic properties in neither monocytes (Figure 11b) nor macrophages (Figure 12d), thereby confirming its immunosuppressive activity and identifying it, for the first time, as a mycotoxin with immunosuppressive properties in immune cells. AST induced a concentration-dependent reduction of NF-κB activity starting already at 0.1 µM (Figure 12c). Decrease in cell viability was observed only at the highest concentration tested of 25 µM. The present results partially align with the study conducted by Partsch et al. (2025), where AST exhibited immunoinhibitory effects (≥2 µM) by suppressing LPS-induced NF-κB activation without causing cytotoxicity [31]. Although the cytotoxic effects of AST were similar in both cell lines, it exhibited a

more pronounced immunoinhibitory effect in macrophages than in monocytes. Furthermore, while all other mycotoxins showed approximately comparable immunosuppressive activity in both THP-1 Lucia^{TM} monocytes and macrophages, AST was also the only compound to elicit immunoinhibitory effects already at concentrations as low as 0.1 µM indicating compound and cell type specificity The differences observed between the results obtained in monocytes and macrophages may be attributed to the intrinsic characteristics of these two cell populations. Although both represent key components of the innate immune system, they differ in origin, functions, and phenotypic features. Differentiation of THP-1 monocytes into macrophages under PMA stimulation is marked by the loss of proliferative capacity, acquisition of adherence, and distinct morphological and phenotypical changes [71]. A study conducted by Takashiba et al. (1999) demonstrated that DNA-binding NF-κB is absent in the cytoplasm of undifferentiated THP-1 cells but accumulates during differentiation. Upon LPS stimulation, NF-κB translocates from the cytoplasm to the nucleus, a process that occurs more rapidly in differentiated cells, which also reach higher final nuclear NF-κB levels compared to undifferentiated cells. These findings suggest that the cytoplasmic accumulation of NF-κB during monocyte-to-macrophage maturation primes the cells for a stronger response to LPS, enabling rapid secretion of inflammatory mediators such as TNF-α by mature macrophages [72].

This further implies that macrophages, due to their higher baseline NF-κB activity following LPS stimulation, may show a more pronounced decrease in NF-κB activity in response to immunosuppressive mycotoxins, resulting in stronger immunosuppressive effects compared to monocytes. However, since the results obtained in this master's thesis are not fully consistent with the findings of Takashiba et al. (1999), future research should aim to clarify the mechanisms underlying these immunomodulatory effects, given that mechanistic studies were not conducted within the scope of this work.

Regarding the mode of action underlying the immunosuppressive effects of TEN and AST so far mechanistic studies have only been conducted for compounds that share structural similarities with AST. Specifically, certain structural resemblances have been identified between AST and *Fusarium* mycotoxins. Kuang et al. (2022) demonstrated that proliferatin suppresses the NF-κB signaling pathway in LPS-stimulated RAW264.7 macrophages. It inhibited the nuclear translocation of NF-κB while simultaneously reducing the phosphorylation of IκBα and IKKα/β [73]. This may represent one of the possible molecular mechanisms underlying the activity of these mycotoxins. However, future research is needed to elucidate the exact mechanisms underlying the immunosuppressive effects of TEN and AST.

In order to understand these immunomodulatory effects more precisely, it is essential to also consider the GIT as the first site of interaction between mycotoxins and the host. The GIT represents the body's first line of defense against harmful substances from food and the environment. IECs are particularly important, as they are the first point of contact with ingested toxins and therefore a crucial focus for research. Their role is not limited to serving as a physical barrier against pathogens, they also actively communicate with immune cells through cytokines and other signaling molecules. This interaction between IECs and immune cells ensures the precise regulation of inflammatory processes, the restoration of homeostasis, and tissue repair. However, when toxins in the gut disrupt this communication, the consequences can be far-reaching: from local impairment of the barrier function and misregulated immune responses to chronic inflammation and lasting tissue damage [49,74,75]. For this reason, the second part of thesis focused on elucidating the immunomodulatory properties of the selected mycotoxins on IECs To this end, qRT-PCR was employed to analyze changes in the expression of pro-inflammatory cytokines (IL-6, IL-8, TNF-α) and the anti-inflammatory cytokine (IL-10) in IL-1β-stimulated, differentiated Caco-2 cells and non-cancerous HCEC-1CT cells. Prior to these experiments, the cytotoxic potential of the mycotoxins was assessed, in order to exclude the possibility that the observed immunosuppressive activity was a consequence of cytotoxicity.

In the present master's thesis, AOH reduced cell viability in IL-1β-stimulated differentiated Caco-2 cells only at the highest tested concentration of 100 µM (Figure 13b). These results are in line with a previously published study, where AOH did not exhibit cytotoxic effects in either IL-1β-stimulated differentiated Caco-2 cells or non-stimulated cells within the tested concentration range (0,02–40 µM) [23]. AOH has also previously been investigated in non-cancerous HCEC-1CT cells, where the WST-1 assay revealed an EC_{50} value of 100.9 µM for AOH when applied in combination with ATX-II. Interestingly, HCEC-1CT cells were reported to be more sensitive to the tested mycotoxins compared to the cancerous HT29 cells [76]. This contrasts with the findings of the present study, in which AOH exhibited similar effects on both the cancerous and non-cancerous cell line (Figure 13b). Some of the discrepancies may be attributed to differences in methodology. Two different assays, namely the CTB and WST-1 assays, were used to assess cytotoxicity. Moreover, one of the most striking differences lies in the fact that the study conducted by Vejdovszky et al. (2017) investigated the combined effects of AOH and ATX-II, which may result in entirely different outcomes compared to testing individual mycotoxins.

To date, the cytotoxic potential of AME has not been evaluated in Caco-2 or HCEC-1CT cells. Therefore, this study represents an important contribution by providing novel insights into the cytotoxic effects of *Alternaria* mycotoxins in both cancerous Caco-2 cells and non-cancerous HCEC-1CT cells. The results demonstrated that AME did not induce cytotoxic effects in Caco-2

cells at the tested concentrations, whereas HCEC-1CT cells exhibited higher sensitivity to this mycotoxin, with a reduction in cell viability observed at concentrations ≥ 5 µM (Figure 13d). These findings are in line with the observations of Vejdovszky et al. (2017), who reported that AME reduced cell viability in the colorectal adenocarcinoma cell line HT29 at concentrations exceeding 25 µM after 24 h of exposure, as determined by the SRB assay [77]. Thus, AME exerts cytotoxic effects on non-immune cells. However, considerable discrepancies between studies may be attributed to methodological differences (e.g., CTB vs. SRB assay), the use of cell lines of different origin (cancerous vs. non-cancerous), as well as variations in exposure duration. In addition, AME has been shown to increase the formation of dichlorofluorescein in HT29 cells, indicating the generation of ROS. This, in turn, leads to modulation of the redox balance through activation of the Nrf2/ARE signaling pathway, but without any apparent negative effect on DNA integrity [77]. This suggests that such modulation may represent one of the molecular mechanisms of action of this *Alternaria* toxin.

In Caco-2 and HCEC-1CT cells, ALT did not exhibit cytotoxicity at the tested concentrations (Figure 13f). Previously the mycotoxin has been investigated in human colorectal adenocarcinoma cells, albeit in a different cell line. In HCT116 cells, ALT was reported to exert cytotoxicity with an IC_{50} value of 3.13 µM following 72 h of incubation. Cytotoxicity was assessed using the SRB assay [78]. As previously noted, the lack of toxicological data obtained from the same cell lines represents a major limitation for the comparison of effects. Therefore, future research should place greater emphasis on Caco-2 and HCEC-1CT cells.

In this study, ALTP reduced viability in Caco-2 cells only at the highest tested concentration of 50 µM, whereas in HCEC-1CT cells it was more potent, inducing cytotoxicity already at 5 µM (Figure 13j). Thus, HCEC-1CT cells were more sensitive to this mycotoxin compared to Caco-2 cells. According to previous reports, ALTP has so far shown cytotoxicity only in HCT116 cells [79]. For the remaining mycotoxins (ATX-I, TEN and AST), knowledge about their cytotoxic effects on IECs is lacking, which therefore represents one of the strengths of the present study and highlights its relevance for future research. ATX-I was more potent in HCEC-1CT cells, showing cytotoxicity at concentrations ≥ 50 µM, whereas in Caco-2 cells, it was cytotoxic only at 200 µM (Figure 13h). TEN were non-cytotoxic in both Caco-2 and HCEC-1CT cells (Figure 13l), while AST was cytotoxic only in HCEC-1CT cells at a concentration of 100 µM (Figure 13n). The results for perylene quinones, ALTP and ATX-I, are in line with previous studies. A structurally related compound, ATX-II, was also found to be significantly more cytotoxic in HCEC-1CT cells compared to HT29 cells, the latter showing the lowest sensitivity to this mycotoxin [76]. Although some mycotoxins exhibit results that do not fully align with the study conducted by Vejdovszky et al. (2017), most mycotoxins displayed markedly higher potency in HCEC-1CT cells compared to Caco-2 cells.

The cytotoxicity of ALTP (Figure 13j), AME (Figure 13d), ATX-I (Figure 13h), and AST (Figure 13n) differed statistically between these two cell lines, with all of which exhibited greater potency in HCEC-1CT cells. In contrast, the remaining tested toxins showed comparable effects in both cell lines. A plausible explanation for this differential sensitivity may lie in differences in metabolism or uptake of the toxins, reflecting the distinct characteristics of cancerous (Caco-2) versus non-cancerous (HCEC-1CT) IECs [76]. Additionally, beyond their origin, these cell lines differ in membrane integrity, which could help explain the divergent results observed in cancerous versus non-cancerous epithelial cells. For example, ATX-II was tested in cancerous HT-29 and non-cancerous HCEC-1CT cells, where even short exposure to this mycotoxin altered the functionality of the cell models. When combined with shear stress, differential responses were observed, particularly in Nrf2 localization. ATX-II reduced migration and membrane fluidity in HCEC-1CT, while having no significant effect on HT-29. In conclusion, ATX-II predominantly disrupts membrane function in HCEC-1CT, compromising their motility/turnover and barrier role [80]. These cell line-specific differences in cytotoxicity highlight the importance of considering cellular context when evaluating the biological activity of *Alternaria* toxins. In line with this, the assessment of their immunomodulatory properties revealed that, among the tested mycotoxins, only ALTP (Figure 14) and AOH (Figure 15) exhibited immunosuppressive effects.

Accordingly, AOH did not reduce IL-6 or IL-8 transcript levels in Caco-2 cells at concentrations ≥ 20 µM; at 30 µM, TNF-α showed a tendency to increase, reaching 1.451 ± 0.199 (Figure 15a). In HCEC-1CT cells, AOH significantly increased TNF-α mRNA from 10 µM (relative transcription 2.096 ± 0.0726) and produced only a modest tendency to reduce IL-8 (Figure 15b). Placing these results in context, earlier work conducted by Schmutz et al. (2019) reported a tendency toward decreased IL-6 and IL-8 in Caco-2 cells above 20 µM and found a stronger TNF-α induction at 40 µM (2.81 ± 0.43), which only partially aligns with our trend at 30 µM for TNF-α [23].

For HCEC-1CT, a previous study described suppression of TNF-α from 1 µM and a concentration-dependent decrease of IL-8 beginning at 1 µM [50], whereas the present data indicate TNF-α induction from 10 µM with only limited effects on IL-8 expression. However, further investigations are necessary to clarify the effects of this mycotoxin on the intestinal epithelial cell lines. Schmutz et al. (2019) suggested that the effects of AOH in Caco-2 cells could be explained by the fact that stimulation of the IL-1β receptor triggers multiple signaling cascades, including activation of NF-κB. Therefore, an AOH-mediated reduction in NF-κB expression could lead to an attenuated response to IL-1β. However, this hypothesis does not explain the TNF-α findings, since TNF-α mRNA levels were significantly increased, indicating that its transcription is mediated by an alternative signaling pathway. Another factor that could play a role is the impact of AOH on miRNA transcript levels, with miR-16 and miR-125b significantly increased at 40 µM AOH. Since

these two miRNAs are generally considered mediators of TNF-α destabilization [23] and could therefore potentially influence the increased transcription levels of TNF-α.

Another important finding of the present study is that ALTP has, for the first time, been characterized as an immunosuppressive compound in non-immune cells (Figure 14a and Figure 14b). The most pronounced decrease in cytokine transcript levels in Caco-2 cells was observed for IL-8 at a concentration of 5 µM, indicating a strong immunosuppressive effect of ALTP, although IL-6 and TNF-α also showed a reduction in transcription levels. IL-10 showed a statistically significant decrease in transcription at 10 µM, but no clear downregulation was observed (Figure 14a). The most pronounced inhibitory effect in HCEC-1CT cells was observed at 2.5 µM ALTP, with a clear reduction in the transcription of all cytokines. Even at 1 µM, the decreases were statistically significant, particularly for IL-6, IL-8, and TNF-α (Figure 14b). When comparing cytokine transcript levels between the two cell lines, a greater reduction in IL-6 expression was observed in HCEC-1CT cells. Based on these findings, it can be concluded that the mechanisms of action are cell-type specific, with more pronounced effects in the non-cancerous cell line. To better understand the underlying mechanisms in IECs, evidence from previous studies suggests that AOH and the perylene quinone ATX-II, structurally related to ALTP, were shown to act on a similar molecular basis. AOH drives nuclear translocation of AhR and Nrf2 and redistributes NF-κB p65, while ATX-II also activates AhR and Nrf2 but does not fully recapitulate AOH's effects in colonic epithelium. In both cases, the increased nuclear-to-cytosolic Nrf2 ratio points to activation of the Nrf2-ARE axis as a likely mediator of their oxidative-stress-related effects [50].

However, oscillations and discrepancies in the results emphasize the necessity for further research to elucidate the mechanisms by which mycotoxins act on non-immune cells and through which signaling mechanisms does the transcription of the tested cytokines operate. Moreover, since these findings are based solely on changes in cytokine mRNA levels, it is essential to validate the observed effects at the protein level in order to confirm that the tested mycotoxin indeed exerts immunosuppressive effects at specific concentrations.

When comparing the results obtained from immune and non-immune cells, it can be concluded that certain mycotoxins induce immunomodulatory effects in immune cells, while similar effects are not observed in IECs for most of the compounds This discrepancy may be explained by the distinct origins and functions of these cellular models. Finally, it can be concluded that natural toxins, such as mycotoxins, have the ability to modulate the immune response, which may result in an impaired capacity of the organism to mount an effective defense against infectious agents. However, an important question arises as to whether the concentrations at which these effects are observed can actually be found in food and thereby influence the immune system of

mammals. Maximum concentrations of certain mycotoxins detected in food, such as AOH, have been shown to reach levels at which immunosuppressive effects may occur. However, for the majority of analyzed food commodities, the concentrations were substantially below these thresholds [12]. Importantly, food is more commonly contaminated with mixtures of multiple mycotoxins rather than a single compound. Such combined exposures may result in significantly stronger effects compared to those elicited by individual toxins alone [29,31]. Consequently, future research should place greater emphasis on elucidating the combined effects of *Alternaria* mycotoxins in order to better assess their potential impact on immune function. The present results demonstrate that certain *Alternaria* mycotoxins exert immunomodulatory effects that contrast with previous assumptions, highlighting the complexity of their biological activity. These findings provide novel insights into the immunosuppressive potential of the selected *Alternaria* mycotoxins and contribute to a deeper understanding of their impact on immune regulation. However, additional studies are required to fully elucidate the underlying molecular mechanisms and to clarify their relevance for human health.

7 Conclusion

This master's thesis investigated the immunosuppressive properties of selected *Alternaria* mycotoxins in both immune and non-immune cells, thereby contributing to the growing understanding of their toxicological relevance. In THP-1 Lucia™ monocytes and macrophages, all tested mycotoxins suppressed LPS-stimulated NF-κB activation. Importantly, ALT and TEN were for the first time identified as immunosuppressive in monocytes, while in macrophages the immunosuppressive activity of AME, ALTP, ATX-I, and AST was demonstrated for the first time. These findings highlight that a broader range of *Alternaria* metabolites than previously known are capable of interfering with innate immune signaling. In addition, ALT and TEN were shown not to induce cytotoxicity in either monocytes or macrophages, whereas AOH, AME, ALTP, ATX-I, and AST reduced cell viability in THP-1 Lucia™ macrophages.

The second part of this thesis focused on non-immune cells. In Caco-2 and HCEC-1CT cells, cytotoxicity and cytokine regulation were assessed to determine the immunomodulatory potential of these compounds. While ALT and TEN were not cytotoxic at the tested concentrations, ALTP and ATX-I reduced cell viability in both cell lines. AME and AST selectively decreased cell viability in HCEC-1CT cells, indicating higher sensitivity of non-cancerous cells. Notably, ALTP was identified for the first time as an immunosuppressive compound in non-immune cells, exerting pronounced effects on both Caco-2 and HCEC-1CT cells. In detail, the perylene quinone ALTP caused a downregulation of IL-8 and TNF-α at 5 µM and of IL-6 at 10 µM in Caco-2 cells, whereas in HCEC-1CT cells the decrease in IL-6, IL-8, and TNF-α transcription started at 1 µM.

In most of the food products examined, the maximum concentrations of *Alternaria* mycotoxins are below the active thresholds that elicit immunomodulatory effects, making it unlikely that biologically relevant levels are reached in the intestinal lumen or blood. Nevertheless, regulatory limits are still lacking for *Alternaria* mycotoxins. Altogether, this work broadens current knowledge on the immunosuppressive and cytotoxic properties of *Alternaria* mycotoxins, some of which are characterized here for the first time. These findings provide novel insights into their potential contribution to food-related health risks. Future studies should focus on molecular mechanisms underlying their activity, as well as on combinatorial effects of mycotoxin mixtures, which are more likely to occur in real dietary exposure scenarios.

8 Supplementary results

The immunomodulatory potential of the remaining tested *Alternaria* mycotoxins, including ALT, AME, ATX-I, TEN, and AST (Figure 16 -Figure 20), was also assessed in IL-1β-stimulated intestinal epithelial cell lines Caco-2 and HCEC-1CT using the qRT-PCR method. These mycotoxins did not show any statistically significant changes, neither a decrease nor an increase in the expression of pro-or anti-inflammatory cytokines (IL-6, IL-8; IL-10 and TNF-α) compared to the positive control (25 ng/ml IL-1β).

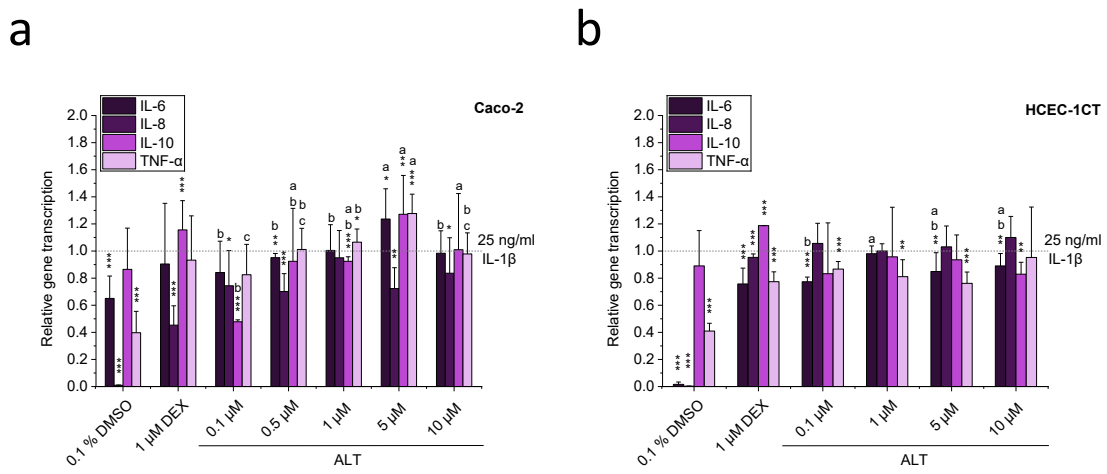

Figure 16: Impact of ALT on relative gene transcription levels of IL-6, IL-8, IL-10 and TNF-α in interleukin 1β (IL-1β) stimulated Caco-2 (a) and HCEC-1CT (b) cells, measured by qRT-PCR. Cells were pre-incubated with ALT or 1 µM dexamethasone (DEX) for 2 h, followed by stimulation with IL-1β (25 ng/ml) for further 3 h. Changes in gene transcript levels are shown as mean + SD of at least three biological replicates, calculated as relative gene transcription ($2^{-\Delta\Delta CT}$), normalized to GAPDH and compared to the positive control (25 ng/ml IL-1β). Student's t-test was used to determine statistically significant differences compared to the positive control (* $p < 0.05$; ** $p < 0.01$; *** $p < 0.001$). One-way ANOVA followed by Fisher's LSD post hoc test was applied to determine statistically significant differences between the different tested concentrations of ALT (a-c; $p < 0.05$).

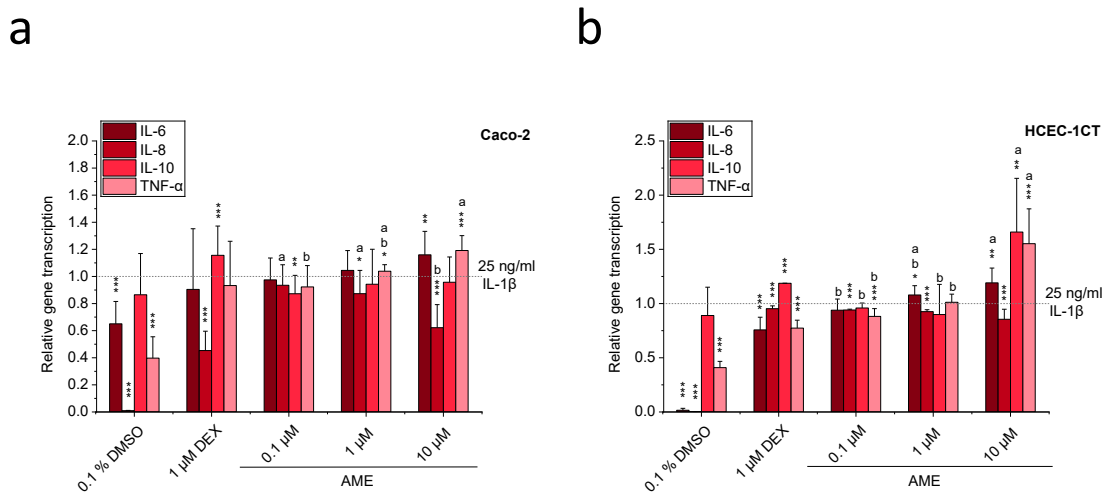

Figure 17: Impact of AME on relative gene transcription levels of IL-6, IL-8, IL-10 and TNF-α in interleukin 1β (IL-1β) stimulated Caco-2 (a) and HCEC-1CT (b) cells, measured by qRT-PCR. Cells were pre-incubated with AME or 1 µM dexamethasone (DEX) for 2 h, followed by stimulation with IL-1β (25 ng/ml) for further 3 h. Changes in gene transcript levels are shown as mean + SD of at least three biological replicates, calculated as relative gene transcription ($2^{-\Delta\Delta CT}$), normalized to GAPDH and compared to the positive control (25 ng/ml IL-1β). Student's t-test was used to determine statistically significant differences compared to the positive control (* $p < 0.05$; ** $p < 0.01$; *** $p < 0.001$). One-way ANOVA followed by Fisher's LSD post hoc test was applied to determine statistically significant differences between the different tested concentrations of AME (a-b; $p < 0.05$).

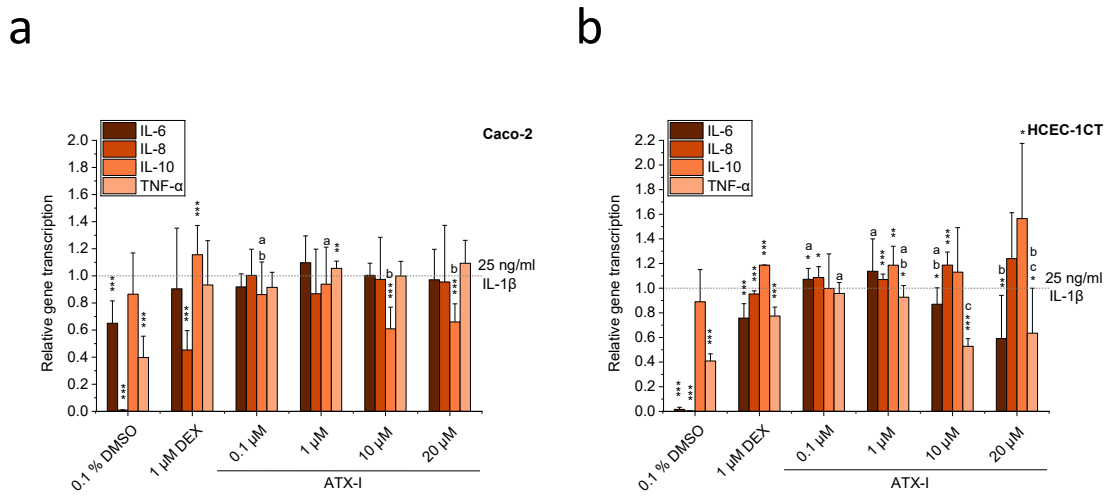

Figure 18: Impact of ATX-I on relative gene transcription levels of IL-6, IL-8, IL-10 and TNF-α in interleukin 1β (IL-1β) stimulated Caco-2 (a) and HCEC-1CT (b) cells, measured by qRT-PCR. Cells were pre-incubated with ATX-I or 1 µM dexamethasone (DEX) for 2 h, followed by stimulation with IL-1β (25 ng/ml) for further 3 h. Changes in gene transcript levels are shown as mean + SD of at least three biological replicates, calculated as relative gene transcription ($2^{-\Delta\Delta CT}$), normalized to GAPDH and compared to the positive control (25 ng/ml IL-1 β). Student's t-test was used to determine statistically significant differences compared to the positive control (* $p < 0.05$; ** $p < 0.01$; *** $p < 0.001$). One-way ANOVA followed by Fisher's LSD post hoc test was applied to determine statistically significant differences between the different tested concentrations of ATX-I (a-c; $p < 0.05$).

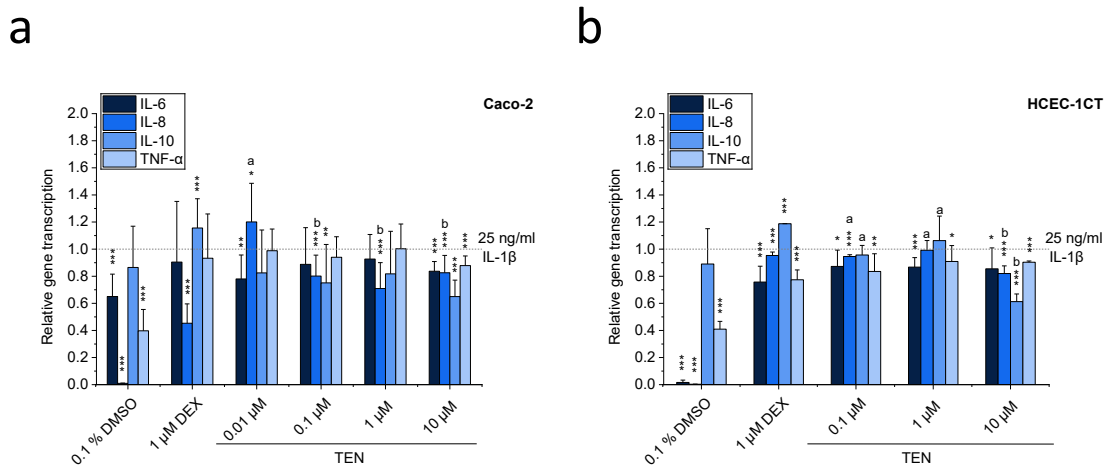

Figure 19: Impact of TEN on relative gene transcription levels of IL-6, IL-8, IL-10 and TNF-α in interleukin 1β (IL-1β) stimulated Caco-2 (a) and HCEC-1CT (b) cells, measured by qRT-PCR. Cells were pre-incubated with TEN or 1 µM dexamethasone (DEX) for 2 h, followed by stimulation with IL-1β (25 ng/ml) for further 3 h. Changes in gene transcript levels are shown as mean + SD of at least three biological replicates, calculated as relative gene transcription ($2^{-\Delta\Delta CT}$), normalized to GAPDH and compared to the positive control (25 ng/ml IL-1β). Student's t-test was used to determine statistically significant differences compared to the positive control (* $p < 0.05$; ** $p < 0.01$; *** $p < 0.001$). One-way ANOVA followed by Fisher's LSD post hoc test was applied to determine statistically significant differences between the different tested concentrations of TEN (a-b; $p < 0.05$).

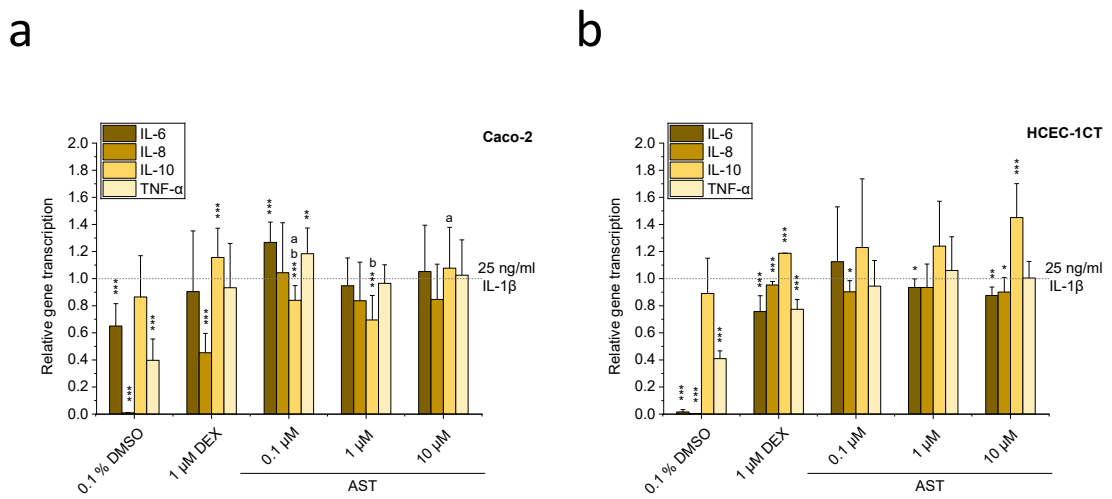

Figure 20: Impact of AST on relative gene transcription levels of IL-6, IL-8, IL-10 and TNF-α in interleukin 1β (IL-1β) stimulated Caco-2 (a) and HCEC-1CT (b) cells, measured by qRT-PCR. Cells were pre-incubated with AST or 1 µM dexamethasone (DEX) for 2 h, followed by stimulation with IL-1β (25 ng/ml) for further 3 h. Changes in gene transcript levels are shown as mean + SD of at least three biological replicates, calculated as relative gene transcription ($2^{-\Delta\Delta CT}$), normalized to GAPDH and compared to the positive control (25 ng/ml IL-1β). Student's t-test was used to determine statistically significant differences compared to the positive control (* $p < 0.05$; ** $p < 0.01$; *** $p < 0.001$). One-way ANOVA followed by Fisher's LSD post hoc test was applied to determine statistically significant differences between the different tested concentrations of AST (a-b; $p < 0.05$).

References

(1) Alshannaq, A.; Yu, J.-H. Occurrence, Toxicity, and Analysis of Major Mycotoxins in Food. *Int. J. Environ. Res. Public. Health* **2017**, *14* (6), 632. https://doi.org/10.3390/ijerph14060632.

(2) Marin, S.; Ramos, A. J.; Cano-Sancho, G.; Sanchis, V. Mycotoxins: Occurrence, Toxicology, and Exposure Assessment. *Food Chem. Toxicol.* **2013**, *60*, 218–237. https://doi.org/10.1016/j.fct.2013.07.047.

(3) Milićević, D. R.; Škrinjar, M.; Baltić, T. Real and Perceived Risks for Mycotoxin Contamination in Foods and Feeds: Challenges for Food Safety Control. *Toxins* **2010**, *2* (4), 572–592. https://doi.org/10.3390/toxins2040572.

(4) Perrone, G.; Ferrara, M.; Medina, A.; Pascale, M.; Magan, N. Toxigenic Fungi and Mycotoxins in a Climate Change Scenario: Ecology, Genomics, Distribution, Prediction and Prevention of the Risk. *Microorganisms* **2020**, *8* (10), 1496. https://doi.org/10.3390/microorganisms8101496.

(5) Turner, N. W.; Bramhmbhatt, H.; Szabo-Vezse, M.; Poma, A.; Coker, R.; Piletsky, S. A. Analytical Methods for Determination of Mycotoxins: An Update (2009–2014). *Anal. Chim. Acta* **2015**, *901*, 12–33. https://doi.org/10.1016/j.aca.2015.10.013.

(6) European Commission. Directorate General for Health and Consumers. *RASFF, the Rapid Alert System for Food and Feed :2012 Annual Report.*; Publications Office: LU, 2013.

(7) *Regulation - 2023/915 - EN - EUR-Lex*. https://eur-lex.europa.eu/eli/reg/2023/915/oj/eng (accessed 2025-08-19).

(8) Gruber-Dorninger, C.; Novak, B.; Nagl, V.; Berthiller, F. Emerging Mycotoxins: Beyond Traditionally Determined Food Contaminants. *J. Agric. Food Chem.* **2017**, *65* (33), 7052–7070. https://doi.org/10.1021/acs.jafc.6b03413.

(9) Meena, M.; Swapnil, P.; Upadhyay, R. S. Isolation, Characterization and Toxicological Potential of Alternaria-Mycotoxins (TeA, AOH and AME) in Different Alternaria Species from Various Regions of India. *Sci. Rep.* **2017**, *7* (1), 8777. https://doi.org/10.1038/s41598-017-09138-9.

(10) Escrivá, L.; Oueslati, S.; Font, G.; Manyes, L. *Alternaria* Mycotoxins in Food and Feed: An Overview. *J. Food Qual.* **2017**, *2017*, 1–20. https://doi.org/10.1155/2017/1569748.

(11) Ostry, V. Alternaria Mycotoxins: An Overview of Chemical Characterization, Producers, Toxicity, Analysis and Occurrence in Foodstuffs. *World Mycotoxin J.* **2008**, *1* (2), 175–188. https://doi.org/10.3920/WMJ2008.x013.

(12) Chain (CONTAM), E. P. on C. in the F. Scientific Opinion on the Risks for Animal and Public Health Related to the Presence of Alternaria Toxins in Feed and Food. *EFSA J.* **2011**, *9* (10), 2407. https://doi.org/10.2903/j.efsa.2011.2407.

(13) Louro, H.; Vettorazzi, A.; López De Cerain, A.; Spyropoulou, A.; Solhaug, A.; Straumfors, A.; Behr, A.-C.; Mertens, B.; Žegura, B.; Fæste, C. K.; Ndiaye, D.; Spilioti, E.; Varga, E.; Dubreil, E.; Borsos, E.; Crudo, F.; Eriksen, G. S.; Snapkow, I.; Henri, J.; Sanders, J.; Machera, K.; Gaté, L.; Le Hegarat, L.; Novak, M.; Smith, N. M.; Krapf, S.; Hager, S.; Fessard, V.; Kohl, Y.; Silva, M. J.; Dirven, H.; Dietrich, J.; Marko, D. Hazard Characterization of Alternaria Toxins to Identify Data Gaps and Improve Risk Assessment for Human Health. *Arch. Toxicol.* **2024**, *98* (2), 425–469. https://doi.org/10.1007/s00204-023-03636-8.

(14) Barkai-Golan, R.; Paster, N. *Mycotoxins in Fruits and Vegetables*; Elsevier, 2011.

(15) Fraeyman, S.; Croubels, S.; Devreese, M.; Antonissen, G. Emerging Fusarium and Alternaria Mycotoxins: Occurrence, Toxicity and Toxicokinetics. *Toxins* **2017**, *9* (7), 228. https://doi.org/10.3390/toxins9070228.

(16) Aichinger, G.; Krüger, F.; Puntscher, H.; Preindl, K.; Warth, B.; Marko, D. Naturally Occurring Mixtures of Alternaria Toxins: Anti-Estrogenic and Genotoxic Effects in Vitro. *Arch. Toxicol.* **2019**, *93* (10), 3021–3031. https://doi.org/10.1007/s00204-019-02545-z.

(17) Authority, E. F. S.; Arcella, D.; Eskola, M.; Gómez Ruiz, J. A. Dietary Exposure Assessment to Alternaria Toxins in the European Population. *EFSA J.* **2016**, *14* (12), e04654. https://doi.org/10.2903/j.efsa.2016.4654.
(18) Solhaug, A.; Eriksen, G. S.; Holme, J. A. Mechanisms of Action and Toxicity of the Mycotoxin Alternariol: A Review. *Basic Clin. Pharmacol. Toxicol.* **2016**, *119* (6), 533–539. https://doi.org/10.1111/bcpt.12635.
(19) Bensassi, F.; Gallerne, C.; Dein, O. S. E.; Hajlaoui, M. R.; Bacha, H.; Lemaire, C. Mechanism of Alternariol Monomethyl Ether-Induced Mitochondrial Apoptosis in Human Colon Carcinoma Cells. *Toxicology* **2011**, *290* (2–3), 230–240. https://doi.org/10.1016/j.tox.2011.09.087.
(20) Pahlke, G.; Tiessen, C.; Domnanich, K.; Kahle, N.; Groh, I. A. M.; Schreck, I.; Weiss, C.; Marko, D. Impact of Alternaria Toxins on CYP1A1 Expression in Different Human Tumor Cells and Relevance for Genotoxicity. *Toxicol. Lett.* **2016**, *240* (1), 93–104. https://doi.org/10.1016/j.toxlet.2015.10.003.
(21) Frizzell, C.; Ndossi, D.; Kalayou, S.; Eriksen, G. S.; Verhaegen, S.; Sørlie, M.; Elliott, C. T.; Ropstad, E.; Connolly, L. An in Vitro Investigation of Endocrine Disrupting Effects of the Mycotoxin Alternariol. *Toxicol. Appl. Pharmacol.* **2013**, *271* (1), 64–71. https://doi.org/10.1016/j.taap.2013.05.002.
(22) Kollarova, J.; Cenk, E.; Schmutz, C.; Marko, D. The Mycotoxin Alternariol Suppresses Lipopolysaccharide-Induced Inflammation in THP-1 Derived Macrophages Targeting the NF-κB Signalling Pathway. *Arch. Toxicol.* **2018**, *92* (11), 3347–3358. https://doi.org/10.1007/s00204-018-2299-4.
(23) Schmutz, C.; Cenk, E.; Marko, D. The *Alternaria* Mycotoxin Alternariol Triggers the Immune Response of IL-1β-stimulated, Differentiated Caco-2 Cells. *Mol. Nutr. Food Res.* **2019**, *63* (20), 1900341. https://doi.org/10.1002/mnfr.201900341.
(24) Grover, S.; Lawrence, C. The Alternaria Alternata Mycotoxin Alternariol Suppresses Lipopolysaccharide-Induced Inflammation. *Int. J. Mol. Sci.* **2017**, *18* (7), 1577. https://doi.org/10.3390/ijms18071577.
(25) Xiao, J.; Zhang, Q.; Gao, Y.-Q.; Tang, J.-J.; Zhang, A.-L.; Gao, J.-M. Secondary Metabolites from the Endophytic *Botryosphaeria Dothidea* of *Melia Azedarach* and Their Antifungal, Antibacterial, Antioxidant, and Cytotoxic Activities. *J. Agric. Food Chem.* **2014**, *62* (16), 3584–3590. https://doi.org/10.1021/jf500054f.
(26) Authority, E. F. S.; Arcella, D.; Eskola, M.; Gómez Ruiz, J. A. Dietary Exposure Assessment to Alternaria Toxins in the European Population. *EFSA J.* **2016**, *14* (12), e04654. https://doi.org/10.2903/j.efsa.2016.4654.
(27) Wang, Y.; Liu, H.-X.; Chen, Y.-C.; Sun, Z.-H.; Li, H.-H.; Li, S.-N.; Yan, M.-L.; Zhang, W.-M. Two New Metabolites from the Endophytic Fungus Alternaria Sp. A744 Derived from Morinda Officinalis.
(28) Schrader, T. J.; Cherry, W.; Soper, K.; Langlois, I.; Vijay, H. m. Examination of Alternaria Alternata Mutagenicity and Effects of Nitrosylation Using the Ames Salmonella Test. *Teratog. Carcinog. Mutagen.* **2001**, *21* (4), 261–274. https://doi.org/10.1002/tcm.1014.
(29) Crudo, F.; Partsch, V.; Braga, D.; Blažević, R.; Rollinger, J. M.; Varga, E.; Marko, D. Discovery of the Alternaria Mycotoxins Alterperylenol and Altertoxin I as Novel Immunosuppressive and Antiestrogenic Compounds in Vitro. *Arch. Toxicol.* **2025**, *99* (1), 407–421. https://doi.org/10.1007/s00204-024-03877-1.
(30) Tran, V. N.; Viktorova, J.; Augustynkova, K.; Jelenova, N.; Dobiasova, S.; Rehorova, K.; Fenclova, M.; Stranska-Zachariasova, M.; Vitek, L.; Hajslova, J.; Ruml, T. In Silico and In Vitro Studies of Mycotoxins and Their Cocktails; Their Toxicity and Its Mitigation by Silibinin Pre-Treatment. *Toxins* **2020**, *12* (3), 148. https://doi.org/10.3390/toxins12030148.
(31) Partsch, V.; Crudo, F.; Piller, D.; Varga, E.; Del Favero, G.; Marko, D. Resolving Complexity: Identification of Altersetin and Toxin Mixtures Responsible for the Immunomodulatory, Antiestrogenic and Genotoxic Potential of a Complex Alternaria Mycotoxin Extract. *Food Chem. Toxicol.* **2025**, *198*, 115315. https://doi.org/10.1016/j.fct.2025.115315.

(32) Akira, S.; Uematsu, S.; Takeuchi, O. Pathogen Recognition and Innate Immunity. *Cell* **2006**, *124* (4), 783–801. https://doi.org/10.1016/j.cell.2006.02.015.
(33) Marshall, J. S.; Warrington, R.; Watson, W.; Kim, H. L. An Introduction to Immunology and Immunopathology. *Allergy Asthma Clin. Immunol.* **2018**, *14* (2), 49. https://doi.org/10.1186/s13223-018-0278-1.
(34) Turvey, S. E.; Broide, D. H. Innate Immunity. *J. Allergy Clin. Immunol.* **2010**, *125* (2), S24–S32. https://doi.org/10.1016/j.jaci.2009.07.016.
(35) Janeway, C. A.; Medzhitov, R. Innate Immune Recognition. *Annu. Rev. Immunol.* **2002**, *20* (1), 197–216. https://doi.org/10.1146/annurev.immunol.20.083001.084359.
(36) Nicholson, L. B. The Immune System. *Essays Biochem.* **2016**, *60* (3), 275–301. https://doi.org/10.1042/EBC20160017.
(37) Liu, T.; Zhang, L.; Joo, D.; Sun, S.-C. NF-κB Signaling in Inflammation. *Signal Transduct. Target. Ther.* **2017**, *2* (1), 17023. https://doi.org/10.1038/sigtrans.2017.23.
(38) Kawai, T.; Akira, S. The Role of Pattern-Recognition Receptors in Innate Immunity: Update on Toll-like Receptors. *Nat. Immunol.* **2010**, *11* (5), 373–384. https://doi.org/10.1038/ni.1863.
(39) Nascimento, C. R.; Rodrigues Fernandes, N. A.; Gonzalez Maldonado, L. A.; Rossa Junior, C. Comparison of Monocytic Cell Lines U937 and THP-1 as Macrophage Models for in Vitro Studies. *Biochem. Biophys. Rep.* **2022**, *32*, 101383. https://doi.org/10.1016/j.bbrep.2022.101383.
(40) *The Impact of Food Bioactives on Health*; Verhoeckx, K., Cotter, P., López-Expósito, I., Kleiveland, C., Lea, T., Mackie, A., Requena, T., Swiatecka, D., Wichers, H., Eds.; Springer International Publishing: Cham, 2015. https://doi.org/10.1007/978-3-319-16104-4.
(41) Mao, H.; Zhao, X.; Sun, S. NF-κB in Inflammation and Cancer. *Cell. Mol. Immunol.* **2025**, 1–29. https://doi.org/10.1038/s41423-025-01310-w.
(42) Biswas, R.; Bagchi, A. NFkB Pathway and Inhibition: An Overview. *Comput. Mol. Biol.* **2016**. https://doi.org/10.5376/cmb.2016.06.0001.
(43) Fagerlund, R.; Kinnunen, L.; Köhler, M.; Julkunen, I.; Melén, K. NF-κB Is Transported into the Nucleus by Importin A3 and Importin A4. *J. Biol. Chem.* **2005**, *280* (16), 15942–15951. https://doi.org/10.1074/jbc.M500814200.
(44) Del Favero, G.; Hohenbichler, J.; Mayer, R. M.; Rychlik, M.; Marko, D. Mycotoxin Alternariol Induces Lipid Peroxidation Connecting Mitochondrial Stress Response to NF-κB Inhibition in THP-1 Macrophages. *Chem. Res. Toxicol.* **2020**, *33* (2), 492–504. https://doi.org/10.1021/acs.chemrestox.9b00378.
(45) Pistol, G. C.; Gras, M. A.; Marin, D. E.; Israel-Roming, F.; Stancu, M.; Taranu, I. Natural Feed Contaminant Zearalenone Decreases the Expressions of Important Pro- and Anti-Inflammatory Mediators and Mitogen-Activated Protein Kinase/NF-κB Signalling Molecules in Pigs. *Br. J. Nutr.* **2014**, *111* (3), 452–464. https://doi.org/10.1017/s0007114513002675.
(46) Woelflingseder, L.; Gruber, N.; Adam, G.; Marko, D. Pro-Inflammatory Effects of NX-3 Toxin Are Comparable to Deoxynivalenol and Not Modulated by the Co-Occurring Pro-Oxidant Aurofusarin. *Microorganisms* **2020**, *8* (4), 603. https://doi.org/10.3390/microorganisms8040603.
(47) Barbara, G.; Barbaro, M. R.; Fuschi, D.; Palombo, M.; Falangone, F.; Cremon, C.; Marasco, G.; Stanghellini, V. Inflammatory and Microbiota-Related Regulation of the Intestinal Epithelial Barrier. *Front. Nutr.* **2021**, *8*, 718356. https://doi.org/10.3389/fnut.2021.718356.
(48) Mörbe, U. M.; Jørgensen, P. B.; Fenton, T. M.; Von Burg, N.; Riis, L. B.; Spencer, J.; Agace, W. W. Human Gut-Associated Lymphoid Tissues (GALT); Diversity, Structure, and Function. *Mucosal Immunol.* **2021**, *14* (4), 793–802. https://doi.org/10.1038/s41385-021-00389-4.
(49) Bouhet, S.; Oswald, I. P. The Effects of Mycotoxins, Fungal Food Contaminants, on the Intestinal Epithelial Cell-Derived Innate Immune Response. *Vet. Immunol. Immunopathol.* **2005**, *108* (1–2), 199–209. https://doi.org/10.1016/j.vetimm.2005.08.010.

(50) Groestlinger, J.; Spindler, V.; Pahlke, G.; Rychlik, M.; Del Favero, G.; Marko, D. *Alternaria Alternata* Mycotoxins Activate the Aryl Hydrocarbon Receptor and Nrf2-ARE Pathway to Alter the Structure and Immune Response of Colon Epithelial Cells. *Chem. Res. Toxicol.* **2022**, *35* (5), 731–749. https://doi.org/10.1021/acs.chemrestox.1c00364.
(51) Del Favero, G.; Zaharescu, R.; Marko, D. Functional Impairment Triggered by Altertoxin II (ATXII) in Intestinal Cells in Vitro: Cross-Talk between Cytotoxicity and Mechanotransduction. *Arch. Toxicol.* **2018**, *92* (12), 3535–3547. https://doi.org/10.1007/s00204-018-2317-6.
(52) Pinton, P.; Nougayrède, J.-P.; Del Rio, J.-C.; Moreno, C.; Marin, D. E.; Ferrier, L.; Bracarense, A.-P.; Kolf-Clauw, M.; Oswald, I. P. The Food Contaminant Deoxynivalenol, Decreases Intestinal Barrier Permeability and Reduces Claudin Expression. *Toxicol. Appl. Pharmacol.* **2009**, *237* (1), 41–48. https://doi.org/10.1016/j.taap.2009.03.003.
(53) Wang, H.; Zhai, N.; Chen, Y.; Fu, C.; Huang, K. OTA Induces Intestinal Epithelial Barrier Dysfunction and Tight Junction Disruption in IPEC-J2 Cells through ROS/Ca2+-Mediated MLCK Activation. *Environ. Pollut.* **2018**, *242*, 106–112. https://doi.org/10.1016/j.envpol.2018.06.062.
(54) Romero, A.; Ares, I.; Ramos, E.; Castellano, V.; Martínez, M.; Martínez-Larrañaga, M.-R.; Anadón, A.; Martínez, M.-A. Mycotoxins Modify the Barrier Function of Caco-2 Cells through Differential Gene Expression of Specific Claudin Isoforms: Protective Effect of Illite Mineral Clay.
(55) Abassi, H.; Ayed-Boussema, I.; Shirley, S.; Abid, S.; Bacha, H.; Micheau, O. The Mycotoxin Zearalenone Enhances Cell Proliferation, Colony Formation and Promotes Cell Migration in the Human Colon Carcinoma Cell Line HCT116. *Toxicol. Lett.* **2016**, *254*, 1–7. https://doi.org/10.1016/j.toxlet.2016.04.012.
(56) Gstraunthaler, G.; Lindl, T. Kultivierung spezieller Zelllinien. In *Zell- und Gewebekultur: Allgemeine Grundlagen und spezielle Anwendungen*; Gstraunthaler, G., Lindl, T., Eds.; Springer: Berlin, Heidelberg, 2013; pp 177–193. https://doi.org/10.1007/978-3-642-35997-2_18.
(57) Bosshart, H.; Heinzelmann, M. THP-1 Cells as a Model for Human Monocytes. *Ann. Transl. Med.* **2016**, *4* (21), 438. https://doi.org/10.21037/atm.2016.08.53.
(58) Sambuy, Y.; Angelis, I. D.; Ranaldi, G.; Scarino, M. L.; Stammati, A.; Zucco, F. The Caco-2 Cell Line as a Model of the Intestinal Barrier: In£uence of Cell and Culture-Related Factors on Caco-2 Cell Functional Characteristics.
(59) Vejdovszky, K.; Warth, B.; Sulyok, M.; Marko, D. Non-Synergistic Cytotoxic Effects of Fusarium and Alternaria Toxin Combinations in Caco-2 Cells. *Toxicol. Lett.* **2016**, *241*, 1–8. https://doi.org/10.1016/j.toxlet.2015.10.024.
(60) Intergovernmental-Oceanographic-Commission-of-UNESCO.Pdf. https://www.researchgate.net/profile/Eileen-Bresnan/publication/284579744_Intergovernmental_Oceanographic_Commission_of_UNESCO/links/568ba32708ae051f9afc5353/Intergovernmental-Oceanographic-Commission-of-UNESCO.pdf#page=29 (accessed 2025-07-12).
(61) *QUANTI-Luc™: Luciferase Detection Reagent*. InvivoGen. https://www.invivogen.com/quanti-luc (accessed 2025-07-30).
(62) *THP-1 Lucia Reporter Cells (NF-κB)*. InvivoGen. https://www.invivogen.com/thp1-lucia-nfkb (accessed 2025-07-30).
(63) Park, K. A.; Byun, H. S.; Won, M.; Yang, K.-J.; Shin, S.; Piao, L.; Kim, J. M.; Yoon, W.-H.; Junn, E.; Park, J.; Seok, J. H.; Hur, G. M. Sustained Activation of Protein Kinase C Down-regulates Nuclear Factor- B Signaling by Dissociation of IKK- and Hsp90 Complex in Human Colonic Epithelial Cells. *Carcinogenesis* **2007**, *28* (1), 71–80. https://doi.org/10.1093/carcin/bgl094.
(64) Lund, M. E.; To, J.; O'Brien, B. A.; Donnelly, S. The Choice of Phorbol 12-Myristate 13-Acetate Differentiation Protocol Influences the Response of THP-1 Macrophages to a pro-Inflammatory Stimulus. *J. Immunol. Methods* **2016**, *430*, 64–70. https://doi.org/10.1016/j.jim.2016.01.012.

(65) CellTiter-Blue(R) Cell Viability Assay Technical Bulletin #TB317. https://www.promega.com/-/media/files/resources/protocols/technical-bulletins/101/celltiter-blue-cell-viability-assay-protocol.pdf?rev=3313091698e544ceaa6fff843658eb84&sc_lang=en (accessed 2025-07-30).
(66) Müller, H.-J.; Prange, D. R. *PCR - Polymerase-Kettenreaktion*, 2. Aufl. 2016.; SpringerLink Bücher; Springer Spektrum: Berlin Heidelberg, 2016. https://doi.org/10.1007/978-3-662-48236-0.
(67) Schmittgen, T. D.; Livak, K. J. Analyzing Real-Time PCR Data by the Comparative CT Method. *Nat. Protoc.* **2008**, *3* (6), 1101–1108. https://doi.org/10.1038/nprot.2008.73.
(68) Yu, Y.; Hou, W.; Liu, Y.; Wang, H.; Dong, L.; Mai, Y.; Chen, Q.; Li, Z.; Sun, S.; Yang, J.; Cao, Z.; Zhang, P.; Zi, Y.; Liu, R.; Gao, J.; Zhang, N.; Li, J.; Ren, L.; Jiang, H.; Shang, J.; Zhu, S.; Wang, X.; Qing, T.; Bao, D.; Li, B.; Li, B.; Suo, C.; Pi, Y.; Wang, X.; Dai, F.; Scherer, A.; Mattila, P.; Han, J.; Zhang, L.; Jiang, H.; Thierry-Mieg, D.; Thierry-Mieg, J.; Xiao, W.; Hong, H.; Tong, W.; Wang, J.; Li, J.; Fang, X.; Jin, L.; Xu, J.; Qian, F.; Zhang, R.; Shi, L.; Zheng, Y. Quartet RNA Reference Materials Improve the Quality of Transcriptomic Data through Ratio-Based Profiling. *Nat. Biotechnol.* **2024**, *42* (7), 1118–1132. https://doi.org/10.1038/s41587-023-01867-9.
(69) Dash, S. P.; Gupta, S.; Sarangi, P. P. Monocytes and Macrophages: Origin, Homing, Differentiation, and Functionality during Inflammation. *Heliyon* **2024**, *10* (8), e29686. https://doi.org/10.1016/j.heliyon.2024.e29686.
(70) Solhaug, A.; Vines, L. L.; Ivanova, L.; Spilsberg, B.; Holme, J. A.; Pestka, J.; Collins, A.; Eriksen, G. S. Mechanisms Involved in Alternariol-Induced Cell Cycle Arrest. *Mutat. Res. Mol. Mech. Mutagen.* **2012**, *738–739*, 1–11. https://doi.org/10.1016/j.mrfmmm.2012.09.001.
(71) Solhaug, A.; Karlsøen, L. M.; Holme, J. A.; Kristoffersen, A. B.; Eriksen, G. S.; Solhaug, A. Immunomodulatory Effects of Individual and Combined Mycotoxins in the THP-1 Cell Line. *Toxicol. In Vitro* **2016**, *36*, 120–132.
(72) Takashiba, S.; Van Dyke, T. E.; Amar, S.; Murayama, Y.; Soskolne, A. W.; Shapira, L. Differentiation of Monocytes to Macrophages Primes Cells for Lipopolysaccharide Stimulation via Accumulation of Cytoplasmic Nuclear Factor kappaB. *Infect. Immun.* **1999**, *67* (11), 5573–5578. https://doi.org/10.1128/IAI.67.11.5573-5578.1999.
(73) Kuang, Q.; Li, Q.; Lei, L.; Wang, Y.; Huang, L.; Dai, Y.-F.; Peng, W.; Zhang, M.; Wang, D.; Gu, Y.; Deng, Y.; Guo, D. Proliferatins Suppress Lipopolysaccharide-Induced Inflammation via Inhibition of the NF-κB and MAPK Signaling Pathways. *Bioorganic Chem.* **2022**, *124*, 105810. https://doi.org/10.1016/j.bioorg.2022.105810.
(74) Thoo, L.; Noti, M.; Krebs, P. Keep Calm: The Intestinal Barrier at the Interface of Peace and War. *Cell Death Dis.* **2019**, *10* (11), 849. https://doi.org/10.1038/s41419-019-2086-z.
(75) Farré, R.; Fiorani, M.; Abdu Rahiman, S.; Matteoli, G. Intestinal Permeability, Inflammation and the Role of Nutrients. *Nutrients* **2020**, *12* (4), 1185. https://doi.org/10.3390/nu12041185.
(76) Vejdovszky, K.; Sack, M.; Jarolim, K.; Aichinger, G.; Somoza, M. M.; Marko, D. *In Vitro* Combinatory Effects of the *Alternaria* Mycotoxins Alternariol and Altertoxin II and Potentially Involved miRNAs. *Toxicol. Lett.* **2017**, *267*, 45–52. https://doi.org/10.1016/j.toxlet.2016.12.011.
(77) Tiessen, C.; Fehr, M.; Schwarz, C.; Baechler, S.; Domnanich, K.; Böttler, U.; Pahlke, G.; Marko, D. Modulation of the Cellular Redox Status by the Alternaria Toxins Alternariol and Alternariol Monomethyl Ether. *Toxicol. Lett.* **2013**, *216* (1), 23–30. https://doi.org/10.1016/j.toxlet.2012.11.005.
(78) Xiao, J.; Zhang, Q.; Gao, Y.-Q.; Tang, J.-J.; Zhang, A.-L.; Gao, J.-M. Secondary Metabolites from the Endophytic *Botryosphaeria Dothidea* of *Melia Azedarach* and Their Antifungal, Antibacterial, Antioxidant, and Cytotoxic Activities. *J. Agric. Food Chem.* **2014**, *62* (16), 3584–3590. https://doi.org/10.1021/jf500054f.
(79) Zhao, D.-L.; Cao, F.; Wang, C.-Y.; Yang, L.-J.; Shi, T.; Wang, K.-L.; Shao, C.-L.; Wang, C.-Y. Alternatone A, an Unusual Perylenequinone-Related Compound from a Soft-Coral-

Derived Strain of the Fungus *Alternaria Alternata*. *J. Nat. Prod.* **2019**, *82* (11), 3201–3204. https://doi.org/10.1021/acs.jnatprod.9b00905.

(80) Del Favero, G.; Zaharescu, R.; Marko, D. Functional Impairment Triggered by Altertoxin II (ATXII) in Intestinal Cells in Vitro: Cross-Talk between Cytotoxicity and Mechanotransduction. *Arch. Toxicol.* **2018**, *92* (12), 3535–3547. https://doi.org/10.1007/s00204-018-2317-6.

List of figures

List of tables

List of equations